

# Myosin I Overexpression Impairs Cell Migration

Kristine D. Novak and Margaret A. Titus

Department of Cell Biology, Duke University Medical Center, Durham, North Carolina 27710

**Abstract.** *Dictyostelium* myoB, a member of the myosin I family of motor proteins, is important for controlling the formation and retraction of membrane projections by the cell's actin cortex (Novak, K.D., M.D. Peterson, M.C. Reedy, and M.A. Titus. 1995. *J. Cell Biol.* 131:1205–1221). Mutants that express a three- to sevenfold excess of myoB (myoB<sup>+</sup> cells) were generated to further analyze the role of myosin I in these processes. The myoB<sup>+</sup> cells move with an instantaneous velocity that is 35% of the wild-type rate and exhibit a 6–8-h delay in initiation of aggregation when placed under starvation conditions. The myoB<sup>+</sup> cells complete the developmental cycle after an extended period of time, but they form fewer fruiting bodies that appear to be small and abnormal. The myoB<sup>+</sup> cells are also deficient in their ability both to form distinct F-actin filled projections such as crowns and to become elongate and polarized. This defect can be attributed to

the presence of at least threefold more myoB at the cortex of the myoB<sup>+</sup> cells. In contrast, threefold overexpression of a truncated myoB that lacks the *src* homology 3 (SH3) domain (myoB/SH3<sup>-</sup> cells) or myoB in which the consensus heavy chain phosphorylation site was mutated to an alanine (S332A-myoB) does not disturb normal cellular function. However, there is an increased concentration of myoB in the cortex of the myoB/SH3<sup>-</sup> and S332A-myoB cells comparable to that found in the myoB<sup>+</sup> cells. These results suggest that excess full-length cortical myoB prevents the formation of the actin-filled extensions required for locomotion by increasing the tension of the F-actin cytoskeleton and/or retracting projections before they can fully extend. They also demonstrate a role for the phosphorylation site and SH3 domain in mediating the *in vivo* activity of myosin I.

CELLULAR extensions such as pseudopodia, lamellipodia, ruffles, and phagocytic cups are required for many eukaryotic cell processes, including translocation and endocytosis. Changes in the cortex beneath the plasma membrane are responsible for creation of such structures, controlling their formation by expanding in some regions to allow protrusions and contracting in others to prevent their formation (Stossel, 1989). The elasticity or tension of the cortical F-actin meshwork is believed to be controlled by proteins that bind and cross-link F-actin, such as filamin, ABP-120,  $\alpha$ -actinin, myosin II, and myosin I (Condeelis, 1993). The role of myosin I in control of the cortical meshwork is of particular interest because of its regulated motor activity and ability to bind membranes as well as F-actin (Pollard et al., 1991). These properties, along with the localization of several forms of myosin I to actin-rich regions such as the cell periphery, the cortex beneath phagocytic cups, filopodia, lamellipodia, and growth cones of many different nonmuscle cell types (Fukui et al., 1989; Baines et al., 1992; Wagner et al., 1992; Ruppert et al., 1993) suggest that this motor protein may mediate the dynamic activity of membrane-associated cortical structures.

The amoeba *Dictyostelium* has been used to investigate the role of myosin I in controlling the cell cortex. *Dictyostelium* is a useful system for studying myosin I function as a wide variety of assays for cytoskeletal function are available and much is known about its F-actin cytoskeleton. Six myosin Is, each encoded by a distinct gene, have been identified in *Dictyostelium*. Three of these are classic myosin Is, myoB, C, and D (Jung et al., 1989, 1993; Peterson et al., 1995), characterized by tail regions containing a polybasic membrane-binding region, an ATP-insensitive actin-binding region (GPA domain), and a *src* homology 3 domain (SH3)<sup>1</sup> (Pollard et al., 1991). Three short myosin Is, myoA, E, and F, have also been identified in *Dictyostelium*. These are characterized by a COOH-terminal tail containing only the polybasic region (Titus et al., 1989, 1995; Urrutia et al., 1993). Immunolocalization studies have demonstrated that myoB, C, and D are concentrated at the leading edge of extending pseudopods during chemotactic locomotion (Fukui et al., 1989; Jung et al., 1993, 1996). The myoB isoform has also been colocalized with F-actin in crownlike membrane extensions during vegetative growth (Novak et al., 1995). The localization of these myosin Is suggests that they play a role in the extension and/or retraction of actin-rich membranous projection.

Address all correspondence to Margaret Titus, Department of Cell Biology, Duke University Medical Center, Durham, NC 27710. Tel.: (919) 681-8859. Fax: (919) 684-5481. E-mail: m.titus@cellbio.duke.edu

1. Abbreviations used in this paper: MIHCK, myosin I heavy chain kinase; nt's, nucleotides; SH3, *src* homology 3 domain.

The ability to target *Dictyostelium* myosin I genes by homologous recombination has provided insight into how myosin I functions in cell movements. For example, null mutants lacking either *myoA* or *myoB* extend a greater number of lateral pseudopods, turn more frequently, and move with a reduced instantaneous cellular velocity (Wessels et al., 1991, 1996; Titus et al., 1993). These results suggested that myosin Is are involved in regulating where and when a cell forms a pseudopod and that this regulation is required for efficient cell motility. *Dictyostelium* mutants lacking two myosin I genes, *myoA*<sup>-</sup>/*myoB*<sup>-</sup> and *myoB*<sup>-</sup>/*myoC*<sup>-</sup>, do not undergo normal cortical rearrangements (Novak et al., 1995). The *Dictyostelium myoA*<sup>-</sup>/*myoB*<sup>-</sup>, *myoB*<sup>-</sup>/*myoC*<sup>-</sup>, and *myoB*<sup>-</sup>/*myoD*<sup>-</sup> myosin I double mutants exhibit decreases in their rates of fluid-phase pinocytosis (Novak et al., 1995; Jung et al., 1996). Actin-filled membrane projections observed in macrophages have been proposed to be important for fluid internalization via macropinocytosis (Swanson and Watts, 1995). If *Dictyostelium* cells undergo fluid-phase pinocytosis by a process similar to that of a macrophage, the reduction in fluid uptake by the myosin I double mutants may be due to an inability to either retract or prevent inappropriate formation of the necessary actin-filled projections (Novak et al., 1995).

Myosin I's activity must be tightly regulated for it to control the timing and position of cellular protrusions. SH3 domains are found in a number of signal transduction proteins, such as phospholipase C and Grb2 (Lowenstein et al., 1992; Mayer and Baltimore, 1993), and in proteins associated with membranes and the actin cytoskeleton, including spectrin and the yeast actin-binding protein ABP1 (Wasenius et al., 1987; Drubin et al., 1990). They have been found to play a key role in mediating protein-protein interactions important for intracellular signaling events. Recently, a 125-kD protein named Acan125 has been shown to associate with the SH3 domain of *Acanthamoeba* myosin IC (Xu et al., 1995). It is possible that a *Dictyostelium* SH3-binding protein may be involved in directing myoB activity.

Another conserved element of the classic myosin I structure that may be important in regulating myosin I actin-based motor function, in addition to the SH3 domain, is a conserved phosphorylation site. The high levels of ameoboid actomyosin I Mg<sup>2+</sup> ATPase, including those of *Dictyostelium myoB* and D, have been shown to require phosphorylation of a single serine or threonine in the head region by a myosin I heavy chain kinase (Côté et al., 1985; Pollard et al., 1991; Lee and Côté, 1995). A consensus phosphorylation sequence site is present in all of the known myosin Is found in lower eukaryotes, as well as in the class VI myosin Is from pig and *Drosophila* (Brzeska and Korn, 1996). Phosphorylation at this site is known to increase myosin activity by changing the conformation of the actin-binding surface loop when in contact with F-actin, which increases Pi release from the ATP-binding site during ATP hydrolysis (Brzeska and Korn, 1996). Cells may use phosphorylation to selectively activate myosin Is and control the timing and location of cortical rearrangements.

One means of exploring the in vivo function of a protein is through the overexpression of the intact protein or one of its domains. The introduction of an excess of a compo-

nent of a multisubunit complex or an increase in the amount of a key player in a cellular function often dramatically alters the process in which it participates (Herskowitz, 1987). For example, the introduction of an excess of phosphodiesterase inhibitor into *Dictyostelium* prestalk cells results in a disruption of the normal morphogenetic events that occur during development (Wu et al., 1995). In COS cells, overexpression of the 50-kD subunit of dynactin, part of the multisubunit complex required for cytoplasmic dynein function, causes cells to accumulate in a prometaphase-like state (Echeverri et al., 1996). The observation that the loss of a myosin I can result in the extension of an increased number of actin-rich processes suggested that an excess of myosin I in the cell would have the opposite effect. Namely, the actin-dependent protrusive activity at the cortex would be inhibited, resulting in cells that could not properly form membrane extensions.

This hypothesis has been tested by creating and analyzing *Dictyostelium* cells that overexpress a classic ameoboid myosin I, myoB. The role of the SH3 domain and the phosphorylation site in controlling myoB activity has also been addressed through the generation of cells that express either an excess of a truncated form of myoB that is lacking the SH3 domain or a mutant form of myoB that contains a point mutation at the consensus phosphorylation site. Analysis of these overexpression strains has provided further insight into the role of myosin I in controlling cellular cortical activity.

## Materials and Methods

### Maintenance of Strains

The parental Ax3 (referred to throughout as wild-type), myoB<sup>+</sup> (full-length myoB-overexpressing transformants), myoB/SH3<sup>-</sup> (truncated myoB-expressing cells), and S332A-myoB (cells expressing a mutant myoB in which serine 332 has been changed to alanine) were all maintained in HL5, either in suspension or on a substrate using standard methods (Spudich, 1982). Suspension cultures were grown in 100 ml HL5 while shaking at 240 rpm. Substrate cultures were grown in 10 ml HL5 on bacteriologic plastic. The myoB<sup>+</sup>, myoB/SH3<sup>-</sup>, and S332A-myoB cultures were maintained in the presence of 10 µg/ml G418 (Geneticin; GIBCO BRL, Gaithersburg, MD).

### Construction of Plasmids

The overexpression plasmid pDTb19 was generated by first removing a 4.2-kb EcoRI/HindIII fragment encompassing the 5' end of myoB from pDTb2 (Novak et al., 1995) and ligating it to EcoRI/HindIII-cut pGEM7 (Promega Corp., Madison, WI), resulting in pDTb10. Next, the PCR was carried out using the 5' primer MYB2, which contains a 5' EcoRI site and a start ATG (5' CCGAATTCATGTCAAAAAAAGTTCAAGCC 3'; nucleotides [nt's] 188–205), and the 3' antisense primer MYB1 (3' CCAC-TAGGTCAACCACCA 5'; nt's 881–898). The resulting PCR product was digested with EcoRI and SnaBI. This product was then ligated to pDTb10, from which the 2.1-kb EcoRI/SnaBI fragment containing the upstream region of myoB had been removed and sequenced to confirm that the PCR did not introduce errors. The resulting plasmid, pDTb12, was then digested with HindIII and ligated to a 1.1-kb HindIII fragment from pDTb2 containing the 3' end of the myoB gene (encompassing the 3' myoB tail region and terminator) to create pDTb16. Finally, pDTb16 was digested with XhoI and incubated with the Klenow fragment of DNA polymerase in the presence of excess deoxynucleotides to fill in the overhanging ends. The 0.3-kb actin 15 promoter from pDRH (Faix et al., 1992) was removed by digestion with BglII and HindIII, treated with Klenow in the presence of excess deoxynucleotide, and ligated to the XhoI-cut pDTb16 to create pDTb18.

The 4.2-kb XbaI/BamHI fragment containing both the actin 15 pro-

motor and the *myoB* coding sequence from pDTb18 was ligated into the XbaI/BamHI-digested vector pFlea, creating pDT619. The pFlea vector contains resistance genes for neomycin and phleomycin, as well as the Ddp1 sequence (a *Dictyostelium* extrachromosomal plasmid origin of replication). It was created by the insertion of a 1.0-kb XbaI fragment encompassing the phleomycin resistance gene from pfeI (Leiting and Noegel, 1991) into the plasmid pSmall. The plasmid pSmall was generated by the excision of a 1.0-kb KpnI fragment from pBig (Patterson and Spudich, 1995).

The vector used to create the *myoB*/SH3<sup>-</sup> cell line, pDTb39, was constructed by first using a PCR to generate a 0.44-kb product spanning the 5' to 3' end of the GPA tail sequence including the HindIII site at nucleotide 3162. This product was amplified using the 5' primer MYBGP5H (5' CCGAATTCTTAAATGCCAAGAATTATAAT 3'; nt's 3131–3145) and the 3' antisense primer MYB22 (3' GGTAGTCTCGTTGAACG-TATTCCTAGGGGG 5'; nt's 3524–3541), which includes a 3' stop codon (underlined) and BamHI site. This PCR fragment was digested with HindIII and BamHI, shortening it to 0.4 kb. The pDTb16 plasmid was digested with HindIII and BamHI, and the 1.0-kb HindIII/BamHI fragment that encompassed the 3' end of the *myoB* coding sequence was removed. The digested PCR product was then ligated to the modified pDTb16 vector to create a 6.4-kb plasmid containing the truncated *myoB* tail. This plasmid was named pDTb34. The region containing the 0.4-kb inserted fragment was sequenced to confirm that no PCR errors were present.

The 0.3-kb actin 15 promoter was excised from pDTb18 by digestion with EcoRI and XbaI and cloned into EcoRI/XbaI-digested pDTb34, placing the promoter 5' to the *myoB* coding sequence and creating pDTb38. The plasmid pDTb38 was then digested with XbaI/BamHI to isolate the 3.4-kb fragment containing the actin 15 promoter and the truncated *myoB* coding sequence. This fragment was ligated to XbaI/BamHI-digested pLittle, another derivative of pBIG (Patterson and Spudich, 1995), to create the *myoB*/SH3-overexpression plasmid pDTb42.

The vector used to create the S332A-*myoB* cell line, pDTb42, was constructed by first using a PCR to create two fragments, each containing a serine to alanine change at amino acid 332 (nt's 1361–1363). The first fragment was made using the 5' oligonucleotide MYB5 (5' CCATTGTTA-GAAGCATTTGG 3'), which spans nucleotides 788 to 807, and the 3' oligonucleotide MYB9 (5' CGTTATAGGTTGCACGACGATTACC 3'), a mutagenic anti-sense primer that spans nucleotides 1349 to 1373 and contains the amino acid change (bold), in a PCR to create a 585-bp fragment. Another PCR fragment was generated in which the 5' mutagenic sense primer, MYB10 (5' GGTAATCGTCGTGCAACCTATAACG 3'), which also spans nucleotides 1349 to 1373 and contained the amino acid change (bold), was combined with the 3' primer, MYB6 (5' GGTCCCATTAATACCTTC 3'), which spanned nucleotides 1649–1668, and used in a PCR to create a 320-bp fragment. The 585 and 320-bp fragments were denatured and allowed to anneal, overlapping at the 585-bp fragment's 3' end and the 320-bp fragment's 5' end. The overlapping region also included the amino acid change.

A primer, made to the middle of the 585-bp fragment (MYB12-5' CAATCCCAATGTTATACAG 3'; nt's 959–980), was combined with MYB6 and the annealed DNA described above to amplify a 700-kb DNA fragment spanning the amino acid change at nucleotide 1361 and two NsiI sites at nucleotides 1250 and 1415. This amplified product was digested with NsiI, and the resulting 161-bp fragment was purified and ligated to NsiI-digested, calf intestinal phosphatase-treated pGEM7 (Promega Corp.) to create the plasmid pDTb21.

The plasmid pDTb22, which contained the full-length *myoB* gene, was digested with NsiI, and the vector was purified away from the 161-bp piece of internal DNA. pDTb21 was then digested with NsiI, liberating the 161-bp fragment containing the serine to alanine mutation. This fragment was then ligated to the NsiI-digested pDTb22 vector. The resulting plasmid, pDTb23, which contained the full *myoB* gene and included the serine to alanine mutation, was sequenced to confirm the proper insertion of the NsiI fragment and the presence of the mutation. The plasmid pDTb23 was digested with XbaI/BamHI to remove the 4.1-kb actin 15 promoter and mutated *myoB* gene and then ligated to XbaI/BamHI digested pLittle to create pDTb42, the S332A-*myoB* overexpression construct.

## *Dictyostelium* Transformations

The transformation of *Dictyostelium* was performed following a slightly modified version (Kuspa and Loomis, 1992) of the original protocol (Howard et al., 1988). 10 µg of intact pDTb19 or pDTb42 plasmid was transformed into Ax3 cells by electroporation, and the cells were allowed to re-

cover overnight in HL5. The cells were then diluted 1:10 into HL5 containing 10 µg/ml G418, and the media were exchanged every third day. Neomycin-resistant colonies were visible by 9 d. 20 independent clones from each transformation were picked and transferred into individual 10-ml plates. Western blot analysis was performed on whole cell lysates that were prepared by resuspension of 1 × 10<sup>6</sup> pelleted cells in urea-containing sample buffer (125 mM Tris, pH 6.8, 6 M urea, 20% glycerol, 4% SDS, 1 mM DTT). For protein samples from streaming cells, 1.5 × 10<sup>7</sup> cells were collected at each time point, pelleted, and lysed in the same sample buffer. The protein concentration was determined by the BioRad DC assay (BioRad Laboratories, Hercules, CA). For each experiment, two identical 6% SDS-PAGE gels were loaded with equal amounts of protein for each sample. One gel was then stained with Coomassie blue, and the other was transferred to nitrocellulose. The nitrocellulose blot was incubated with a polyclonal antibody generated against *myoB* (Novak et al., 1995), followed by incubation with an HRP-conjugated goat anti-rabbit secondary antibody (BioRad Laboratories). Antibody reactivity was visualized by enhanced chemiluminescence (Amersham Corp., Arlington Heights, IL).

Films from the Western blots were scanned using a color scanner (model ES1200C; Epson, Pittsburgh, PA). The scanned images were then imported into NIH Image 1.54 (Bethesda, MD), and the mean pixel values of the *myoB* reactive bands were measured. These values were used to determine relative expression levels for each sample. Serial dilutions of Ax3 lysates were included on each Western blot to confirm that autoradiograms used for quantification were within the linear range. The full-length and truncated *myoB*-overexpressing cells were named HTD8, HTD9, and HTD10, respectively. These are referred to by their colloquial names, *myoB*<sup>+</sup>, *myoB*/SH3<sup>-</sup>, and S332A-*myoB* throughout the paper.

## Assays

Pinocytosis of cells in suspension culture was carried out using FITC-dextran as described by others (Klein and Satre, 1986). Fluorescence was measured on a fluorescence spectrophotometer (model 650-40; Perkin-Elmer Corp., Norwalk, CT) with an excitation wavelength of 470 nm and emission wavelength of 520 nm. A standard curve was used to calculate µl FITC-dextran/10<sup>6</sup> cells.

The localization of F-actin was examined in suspension-grown Ax3, *myoB*<sup>+</sup>, *myoB*/SH3<sup>-</sup>, and S332A-*myoB* cells that were allowed to adhere to a 22-mm coverslip for 10 min. The F-actin distribution was observed by staining cells with rhodamine-phalloidin (Molecular Probes, Eugene, OR) following a previously described procedure (Peterson et al., 1995). Confocal microscopy was performed using a laser scanning confocal microscope (model Axiovert; Carl Zeiss, Inc., Thornwood, NY) with a 63× objective (1.25 NA).

Immunofluorescent localization of *myoB* was performed using suspension-grown Ax3, *myoB*<sup>+</sup>, *myoB*/SH3<sup>-</sup>, and S332A-*myoB* cells that were allowed to adhere to coverslips for 15 min. The cells were then fixed immediately for 5 min in -10°C MeOH/1% formaldehyde. The coverslips were washed in PBS and then incubated for 30 min at 37°C with the *myoB* antibody (Novak et al., 1995). The coverslips were washed again in PBS and incubated for 30 min at 37°C with FITC-labeled goat anti-rabbit antibody (BioRad Labs). After washing again with PBS, the coverslips were mounted in 50% glycerol in PBS with 0.1 gm/ml DABCO (Sigma Chemical Co., St. Louis, MO), sealed, and analyzed by laser scanning confocal microscopy as for the rhodamine-phalloidin analysis.

The streaming and development assays were performed as previously described (Jung and Hammer, 1990; Peterson et al., 1995). Streaming cells were observed on a microscope (model Axiovert; Carl Zeiss, Inc.) using a 10× objective (0.3 NA) with a 1.25× optivar lens, or a 20× objective (0.5 NA) and a 2× optivar lens. Images were captured into IP Lab software (Signal Analytics Corp., Vienna, VA) using a camera (model Star 1; Photonics Ltd., Tucson, AZ). Random fields of cells were photographed at 40× magnification and were used to measure the average length of the cells during streaming. The cells were measured along their longest axis, and the average value and standard deviation were determined for each strain.

Cells were developed on MES agar as previously described (Peterson et al., 1995). Images were obtained on a dissecting scope (model Wild M28; Leica, Inc., Deerfield, IL) with a 5× objective and then captured and digitized using a CCD (model 3; Sony Corp., Park Ridge, NJ) camera and Capture+ software (NuVista Inc., Indianapolis, IN). The number of fruiting bodies per cm<sup>2</sup> was determined after allowing an equal number of Ax3 or *myoB*<sup>+</sup> cells to undergo development on nonnutrient agar as previously described (Peterson et al., 1995). At 40 h after starvation, a grid containing 1-cm squares was placed under each plate of fully developed cells. Using a

dissecting microscope (Advanced Imaging Concepts, Princeton, NJ) with a 2× objective lens and an 8× optivar lens, the number of fruiting bodies per square were counted for 50 squares from each plate. An average number was determined for each cell line.

The instantaneous velocity measurements were taken from mid log-phase Ax3 and myoB<sup>+</sup> cells undergoing streaming (Jung and Hammer, 1990; Peterson et al., 1995). At the preaggregation stage (determined by the formation of concentric circles of cells in the center of the cell carpet) (Varnum et al., 1986), cells were collected and diluted 10-fold in MES buffer (20 mM MES, pH 6.8, 2 mM MgSO<sub>4</sub>, 0.2 mM CaCl<sub>2</sub>). Before cell collection, cells at the edge of the plate that were slightly ahead in development were removed by vacuum suction. The diluted cells were allowed to attach to coverslips for 5 min and then viewed on an upright microscope (model Axioplan; Carl Zeiss, Inc.) using a 10× objective (0.3 NA) and a 3× optivar lens. Videotapes of crawling cells were made with a Sony Super VHS videorecorder and recorded onto Maxell XRS-Black super VHS videotape (Fairlawn, NJ). Instantaneous velocity measurements were made using the Real Time Measurement System as previously described (Peterson et al., 1995).

Triton-insoluble cytoskeletons and Triton-soluble fractions of cells were isolated as described (Egelhoff et al., 1991). Triton-soluble and insoluble fractions from a total of 1.5 × 10<sup>6</sup> cells from each strain were separated in a buffer containing 0.1 M MES buffer, pH 6.8, 2.5 mM EGTA, 5 mM MgCl<sub>2</sub>, and 0.5 mM Mg<sup>2+</sup> ATP. The total pellet from each fraction was resuspended in the SDS gel sample buffer described above, run on SDS-PAGE gels, and either transferred to nitrocellulose filters for Western blot analysis (described above) or stained with Coomassie blue. The Coomassie-stained gels and autoradiographs were scanned as described above. The mean pixel values for each lane of the Coomassie-stained gel were determined using NIH Image 1.54 to confirm that the samples were equally loaded. The mean pixel values were then used to standardize the intensity of the myoB bands on the autoradiographs for each sample.

Scanning electron microscopy was performed on the Ax3, myoB<sup>+</sup>, myoB/SH3<sup>-</sup>, and S332A-myoB cells that were grown in suspension cultures and allowed to adhere to Thermanox coverslips 10–15 min before fixation. Cells were processed and analyzed as previously described (Novak et al., 1995).

## Results

### Overexpression of the myoB Heavy Chain

*Dictyostelium* cells expressing an excess of a full-length classic ameboid myosin I, myoB (Fig. 1 A), were created by transformation of Ax3 cells with the expression vector pDTb19, an extrachromosomal plasmid that has the gene for neomycin resistance and uses the actin 15 promoter to drive the expression of the *myoB* gene. Three independent transformations with this construct each generated over 50 colonies resistant to neomycin. 20 colonies from each transformation were subcloned and myoB expression levels were determined by a quantitative immunoblot analysis. The individual clones were found to express three- to sevenfold higher levels of myoB than the parental Ax3 cells (Fig. 1 B). The high expression level of the myoB heavy chain in myoB<sup>+</sup> clones was maintained for ~3 wk after transformation. The myoB expression levels decreased with cell passage after this time, eventually reaching wild-type levels (note that the cells were still resistant to G418). When the myoB expression reached wild-type levels, the behavior of the cells reverted to normal, i.e., the cells behaved identically to Ax3 in all assays (data not shown). Therefore, all experiments were performed on cells that had not been passaged for more than 3 wk, and the myoB expression levels were checked before each experiment. A total of three independent myoB<sup>+</sup> clones (one from each transformation, two of which expressed a threefold excess of myoB, and one that expressed a seven-

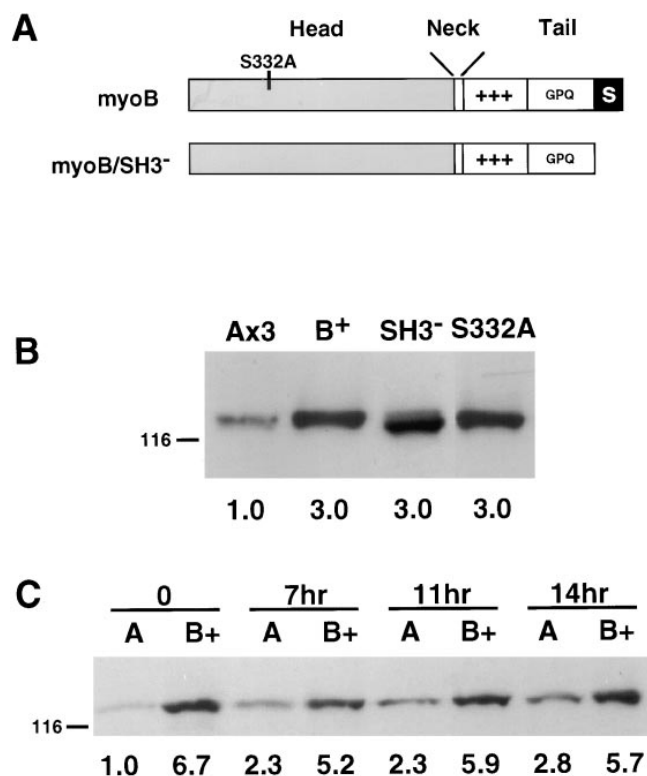


**Figure 1.** The myoB<sup>+</sup> cells express an excess of myoB. Western blot analysis of total cell lysates was used to determine the expression level of the myoB heavy chain in wild-type and overexpression strains. The position of the 116 kD molecular mass marker is indicated on the left of Western blot panels B and C. (A) Box diagram illustrating the major structural elements of the *Dictyostelium* myoB heavy chain and the truncated form, myoB/SH3<sup>-</sup>. The gray box represents the NH<sub>2</sub>-terminal 820 amino acid Head domain, and the Neck region consists of a single IQ motif, the site of presumed light chain binding. In the COOH-terminal tail region: +, the polybasic membrane-binding domain; GPQ, GPQ domain; S, the SH3 domain; S332A, the phosphorylation site at serine 332. (B) The levels of expression of the 125-kD myoB heavy chain in Ax3 control (Ax3), the myoB<sup>+</sup> overexpression strain (B<sup>+</sup>), the myoB/SH3<sup>-</sup> overexpression strain (SH3<sup>-</sup>), and the myoB serine to alanine mutant overexpression strain (S332A). The levels of myoB expression are shown below each lane, and the values are expressed relative to the Ax3 strain (which is set to 1). The myoB antibody recognizes the endogenous myoB as well as the smaller truncated myoB in the myoB/SH3<sup>-</sup> cells and the mutant form of myoB in the S332A-myoB cells. (C) The levels of myoB in the myoB<sup>+</sup> cells remain elevated throughout streaming. A representative Western blot of Ax3 cells (lanes A) and myoB<sup>+</sup> cells (lanes B<sup>+</sup>) during streaming. The time at which the samples were taken are indicated above lanes. The level of myoB expression in the myoB<sup>+</sup> cells relative to that expressed in the Ax3 cells at 0 time (which is set to 1.0) is shown beneath each lane.

fold excess) were analyzed in detail, and the behavior of each was found to be identical.

### Overexpression of Truncated and Mutated myoB Heavy Chains

A second series of *Dictyostelium* transformants that expressed a truncated form of the myoB heavy chain lacking

the COOH-terminal 54 amino acids comprising the SH3 domain was created to investigate the role of the SH3 domain in localization and function of myosin I. A third series of transformants was created that expressed a mutant form of myoB in which serine 332, the consensus phosphorylation site, had been mutated to alanine, mimicking the unphosphorylated form of myoB. To create these mutant myoB-expressing cell lines, wild-type Ax3 cells were transformed with the expression plasmid pDTb42, an extrachromosomal plasmid that has the gene for neomycin resistance and uses the actin 15 promoter to drive the expression of the SH3 truncation of *myoB* gene, or pDTb43, which contains the same selectable marker and actin 15 promoter driving expression of myoB with the serine 332 to alanine change. A total of 20 colonies were collected and analyzed for the presence of the excess myoB heavy chain. (They were referred to as myoB/SH3<sup>-</sup> cells or S332A-myoB cells.) Western blot analysis of the myoB/SH3<sup>-</sup> cell lysates demonstrated that the myoB polyclonal antibody recognized the full-length (~125 kD) endogenous myoB protein, as well as a smaller, truncated myoB heavy chain (~119 kD; Fig. 1 B). Quantification of the Western blots revealed the myoB/SH3<sup>-</sup> and S332A-myoB clones analyzed each expressed threefold more of the mutant protein than endogenous myoB (Fig. 1 B). These levels of overexpression were identical to that of the myoB<sup>+</sup> cells. Three independent clones, all overexpressing a three to fivefold excess of mutant myoB, were analyzed for each cell type and were found to behave identically in all of the experiments described below.

### ***MyoB Overexpression Affects Cell Motility and Development***

*Dictyostelium* cells undergoing starvation begin a process known as “streaming” that corresponds to the early aggregation stages of development. Previous studies have demonstrated that cells lacking one or more myosin Is exhibit delays in streaming while submerged in starvation buffer (Jung and Hammer, 1990; Novak et al., 1995; Peterson et al., 1995; Jung et al., 1996). The Ax3 (control) cells became elongate and began streaming into aggregation centers by 8–9 h when placed in starvation buffer (Fig. 2 A). Mound formation was detected by 11 h (Fig. 2 D), and the cells were fully aggregated into compact mounds by 14 h (Fig. 2 G). The *myoB*<sup>-</sup> mutant cells began to become elongate at 9 h (Fig. 2 B), were observed to undergo streaming into aggregation centers at 11 h (Fig. 2 E), and began forming mounds at 14 h (Fig. 2 H). In contrast, the myoB<sup>+</sup> cells were still round at 9 and 11 h after starvation and required up to 14 h to begin streaming into aggregation centers (Fig. 2 I). myoB<sup>+</sup> cells did not form mounds until after 18–20 h of starvation (data not shown). We also observed many myoB<sup>+</sup> cells that did not join in the streams, but remained behind as individual cells (Fig. 2 J).

The delay in streaming between the myoB<sup>+</sup> and Ax3 cells was reflected in their different morphologies observed at higher magnification (Fig. 3). At the time when the control Ax3 cells began to stream (8–9 h after starvation), cells in the stream and those moving toward it are highly elongate (Fig. 3, A and B). The myoB<sup>+</sup> cells that had reached an equivalent stage (14 h after starvation)

were also closely observed. Even though the myoB<sup>+</sup> cells do form aggregation streams, most of the cells both in and around the streams are not as elongate as Ax3 cells, and most were still round (Fig. 3, C and D). Highly elongate cells like those observed in the Ax3 streams were not observed at any point up to or during the streaming process (data not shown). The average length along the long axis of the cells during streaming was measured to confirm this impression. The Ax3 cells 8 h after starvation had an average length of 26.8  $\mu\text{m}$  ( $\pm 6.5 \mu\text{m}$ ;  $n = 53$ ), and the myoB<sup>+</sup> cells 14 h after starvation exhibited an average length of 9.83  $\mu\text{m}$  ( $\pm 4.5 \mu\text{m}$ ;  $n = 83$ ).

Cells overexpressing the myoB/SH3<sup>-</sup> and the S332A-myoB forms of myoB were also tested in the streaming assay (Fig. 4). Both myoB/SH3<sup>-</sup> (Fig. 4 B) and S332A-myoB (Fig. 4 C) cells began to form aggregation streams 8 h after starvation, identically to Ax3 cells (Fig. 4 A). These cells were observed to become highly elongate as they moved into the aggregation streams and completed mound formation in the normal time frame (12–14 h, data not shown).

The observed differences in the amount of time required for streaming by the myoB<sup>+</sup> cells led us to determine their instantaneous velocity. The velocity of *Dictyostelium* cells has been shown to vary at different time points throughout the developmental program (Varnum et al., 1986), reaching a peak at the initial aggregation stage. We measured the instantaneous velocities of Ax3 and myoB<sup>+</sup> cells at this stage, using the streaming assay to directly observe the cells. In the streaming assay, Ax3 cells remained as a smooth carpet of cells until 6 h after starvation, when aggregation was initiated, as determined by “rippling” of the cell carpet (Varnum et al., 1986). Aggregation-stage Ax3 cells were collected and used for instantaneous velocity measurements. The onset of the myoB<sup>+</sup> cell aggregation was not observed until 11 h after starvation, the time point at which these cells were collected and measured. Ax3 instantaneous velocity was found to be  $17.43 \pm 5.86 \mu\text{m}/\text{min}$  ( $n = 27$ ), and the myoB<sup>+</sup> instantaneous velocity was  $6.65 \pm 4.6 \mu\text{m}/\text{min}$  ( $n = 31$ ).

The levels of the myoB heavy chain protein in the Ax3 and myoB<sup>+</sup> cells were compared throughout the streaming time course to determine the relationship between myoB protein levels and the initiation of streaming. Transcriptional activation by the actin 15 promoter, the promoter used to overexpress myoB in these studies, has been shown to be developmentally regulated. Maximal levels of expression from this promoter are observed between 2 and 6 h after starvation, with a significant decrease in transcriptional activity occurring between 6 and 12 h after starvation (Cohen et al., 1986). The level of the myoB heavy chain present in the Ax3 control cells was found to increase during the streaming assay (Fig. 1 C, lanes marked A). Quantification of the blot revealed that the myoB levels in Ax3 cells increased by almost threefold by 14 h (Fig. 1 C, compare A lanes). The myoB<sup>+</sup> cells were found to express approximately the same relative level of myoB heavy chain from the beginning to the end of the streaming assay (Fig. 1 C, lanes marked B<sup>+</sup>). The absolute excess of myoB in the myoB<sup>+</sup> cells relative to the Ax3 cells was found to decrease between the onset of starvation and 7 h, remaining at 2 to 2.6-fold until the cells began to stream at 14 h (Fig. 1 C). The initiation of streaming by the myoB<sup>+</sup>

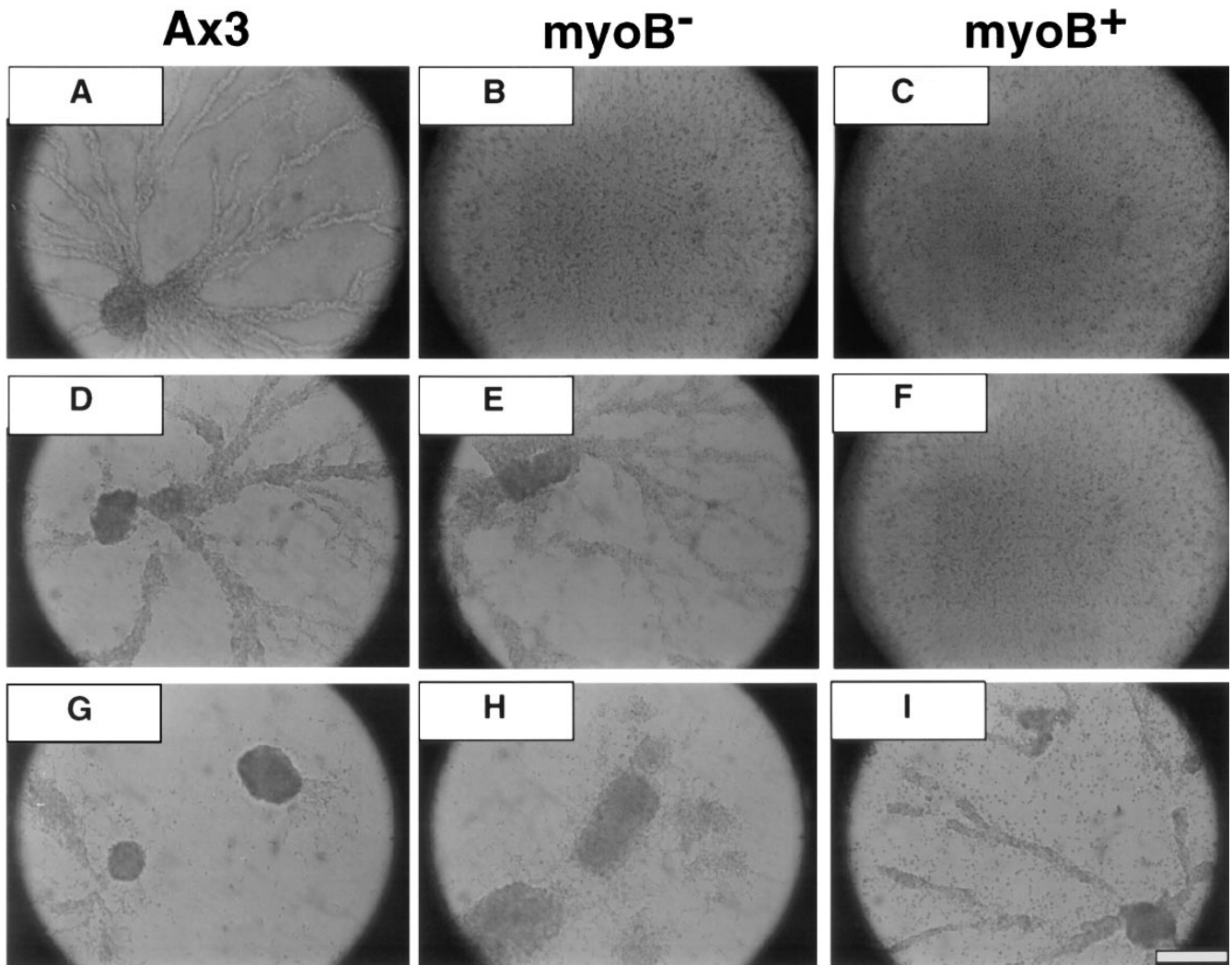


**Figure 2.** The expression of an excess of *myoB* affects the early aggregation stages of *Dictyostelium* development. A streaming assay was employed to examine the motility of the *myoB*<sup>+</sup> cells during aggregation. The Ax3 (A, D, and G), *myoB*<sup>-</sup> null (B, E, and H), and *myoB*<sup>+</sup> cells (C, F, and I) were submerged in starvation buffer and photographed at 9 h (A, B, and C), 11 h (D, E, and F) or 14 h (G, H, and I). Bar, 100  $\mu$ m.

cells at 14 h, therefore, did not strictly correlate with a drop in the levels of *myoB*.

The full developmental program of *myoB*<sup>+</sup> cells was observed on nonnutrient agar. The Ax3 cells aggregated to form compact, round mounds within 8 h (Fig. 5 A) and were fully developed into fruiting bodies by 24 h (data not shown). The *myoB*<sup>+</sup> cells were still undergoing aggregation 12 h after starvation (Fig. 5 B). The *myoB*<sup>+</sup> cells had only reached the early stalk stage of development after 24 h of starvation (data not shown) and required over 36 h to complete development and form mature fruiting bodies (Fig. 5 D). Although the fully developed *myoB*<sup>+</sup> cells do produce viable spores, the final fruiting bodies themselves were much smaller than Ax3, even 40 h after starvation (compare Fig. 5, C and D, arrows), and many cells appeared to be left behind on the plate as individual cells (not observable in figure) or in undeveloped mounds (Fig. 5 D, star).

A count of the number of mature fruiting bodies on

nonnutrient agar plated with an equal number of cells revealed that Ax3 cells averaged 31.5 fruiting bodies per cm<sup>2</sup>, while *myoB*<sup>+</sup> cells averaged 3.7 fruiting bodies per cm<sup>2</sup>. The delay in the onset of aggregation and an inability to undergo shape changes required for maximal motility may be responsible for these developmental abnormalities. No defects or delays in development were observed with the *myoB*/SH3<sup>-</sup> or S332A-*myoB* cells. The *myoB*/SH3<sup>-</sup> cells were able to undergo normal development; these cells produced normal numbers of full-size fruiting bodies with viable spores in the same time frame as Ax3 cells (data not shown).

#### *MyoB Is Accumulated in the Cortex of the myoB<sup>+</sup> and myoB/SH3<sup>-</sup> Cells*

The abnormal morphology of the streaming *myoB*<sup>+</sup> cells suggested that excess *myoB* was interfering with the activities at the cortex of these cells. This was assessed by ana-

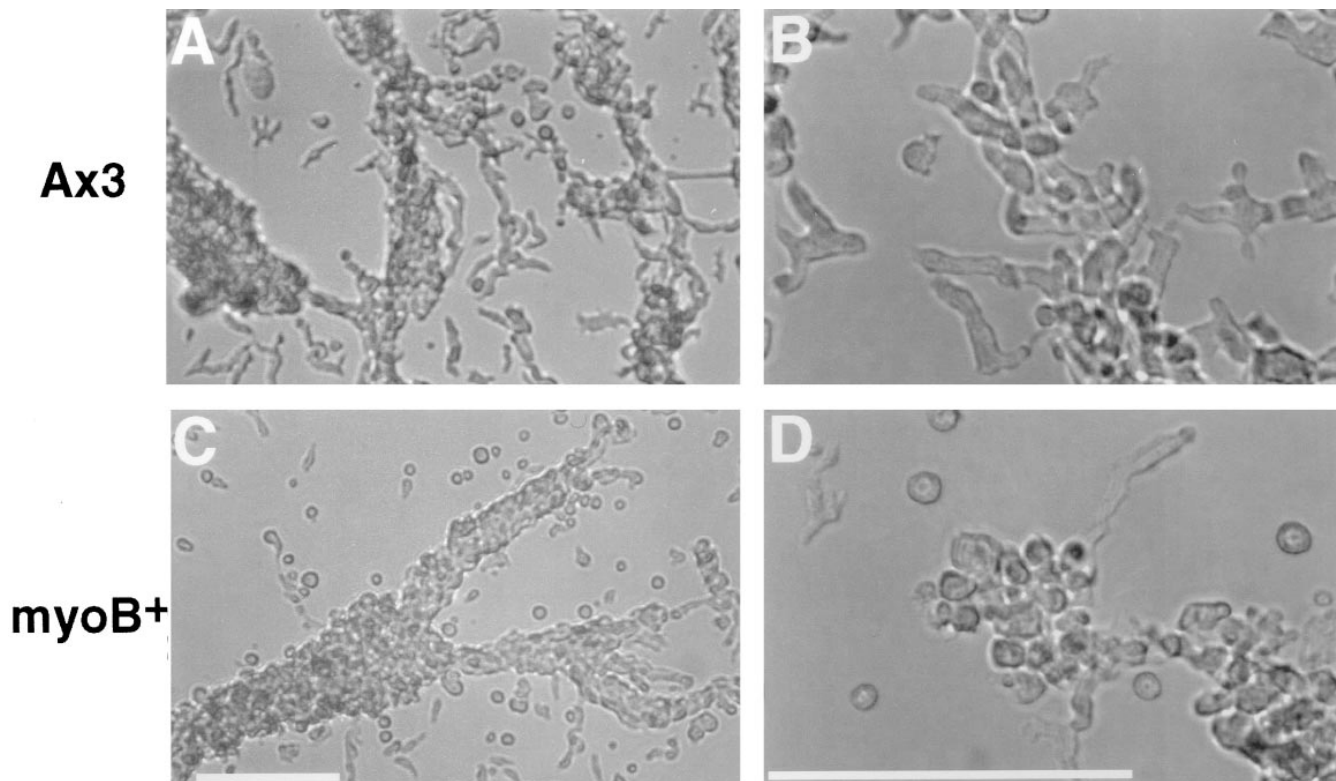


**Figure 3.** The myoB<sup>+</sup> cells are morphologically different during aggregation. Shown are DIC micrographs of Ax3 cells (*A* and *B*) and myoB<sup>+</sup> cells (*C* and *D*) during the streaming process (8 h for the Ax3 cells and 14 h for the myoB<sup>+</sup> cells). The cells were photographed at both low (12×; *A* and *C*) and high (40×; *B* and *D*) magnification to show cell shape differences between the two cell lines during streaming. Bars, 100 μm.

lyzing Triton-insoluble cytoskeletons (Spudich, 1987; Egelhoff et al., 1991) prepared from an equal number of Ax3, myoB<sup>+</sup>, myoB/SH3<sup>-</sup>, and S332A-myoB cells. Comparison of the Triton-insoluble fraction with the Triton-soluble fraction resolved on SDS-PAGE gels revealed that the majority of the myoB was present in the Triton-soluble fraction in the Ax3, myoB<sup>+</sup>, myoB/SH3<sup>-</sup> cells, and S332A-myoB (Fig. 6 *B*, lanes marked *s*).

Quantitative immunoblotting revealed that only slightly more myoB (1.5-, 2.5-, and 1.8-fold, respectively) was present in the Triton-soluble fraction of the myoB<sup>+</sup>, myoB/SH3<sup>-</sup>, and S332A-myoB cells than in that of the Ax3 cells. Only 7% of the cell's total myoB was found in the insoluble cytoskeleton of Ax3 cells (Fig. 6, *first and second lanes*). A 7.2-fold increase in the amount of myoB was found in the Triton X-100 pellet of the myoB<sup>+</sup> cells, corresponding to 24% of the cell's total myoB (Fig. 6 *B*, *third and fourth lanes*). There was a 5.3-fold excess of truncated myoB present in the Triton-insoluble fraction of the myoB/SH3<sup>-</sup> cells, representing 20% of the total myoB (Fig. 6 *B*, *sixth lane*), and 5.2-fold more mutated myoB present in the Triton-insoluble cytoskeletons of the S332A-myoB cells, representing 20% of the total myoB (Fig. 6, *eighth lane*). These results demonstrate that there is an excess amount of both the full-length as well as the truncated and mutant myoB heavy chain present in the Triton-insoluble cytoskeleton in all three cell types. However, only the excess of full-length myoB protein affects the behavior of the cell.

Immunolocalization of myoB was performed to determine its intracellular distribution in each of the cell lines after attachment to a substrate for 15 min. The control Ax3 cells were found to have diffuse fluorescence in the cytoplasm, with small amounts visible at the periphery, and in small cellular projections (Fig. 7 *A*, *arrow*). This is in agreement with previously published images of the myoB distribution in vegetative cells (Novak et al., 1995) and differs from the localization pattern observed in cells undergoing directed chemotaxis (Fukui et al., 1989). Consistent with the results obtained from analysis of Triton X-100-insoluble cytoskeletons (Fig. 6), the myoB distribution in myoB<sup>+</sup> cells appeared to be quite different from that of the Ax3 cells. A bright band of myoB staining appeared all around the periphery of the myoB<sup>+</sup> cells in addition to the observed cytoplasmic staining (Fig. 7 *B*, *arrow*; compare with Ax3 in Fig. 7 *A*). Immunofluorescent localization of myoB in the myoB/SH3<sup>-</sup> cells revealed that even though these cells did not exhibit the myoB<sup>+</sup> phenotype, the total myoB protein was localized in the same manner as observed for the myoB<sup>+</sup> cells (Fig. 7 *C*). While myoB was present in the cytoplasm of the myoB/SH3<sup>-</sup> cells, bright staining was also clearly visible around the periphery of each cell (Fig. 7 *C*, *arrow*). Many S332A-myoB cells were also observed to possess the bright border staining (Fig. 7 *D*, *arrow*), but S332A-myoB cells were also observed in which the myoB localization was primarily cytoplasmic, with bright spots at the periphery (Fig. 7 *D*, *stars*).

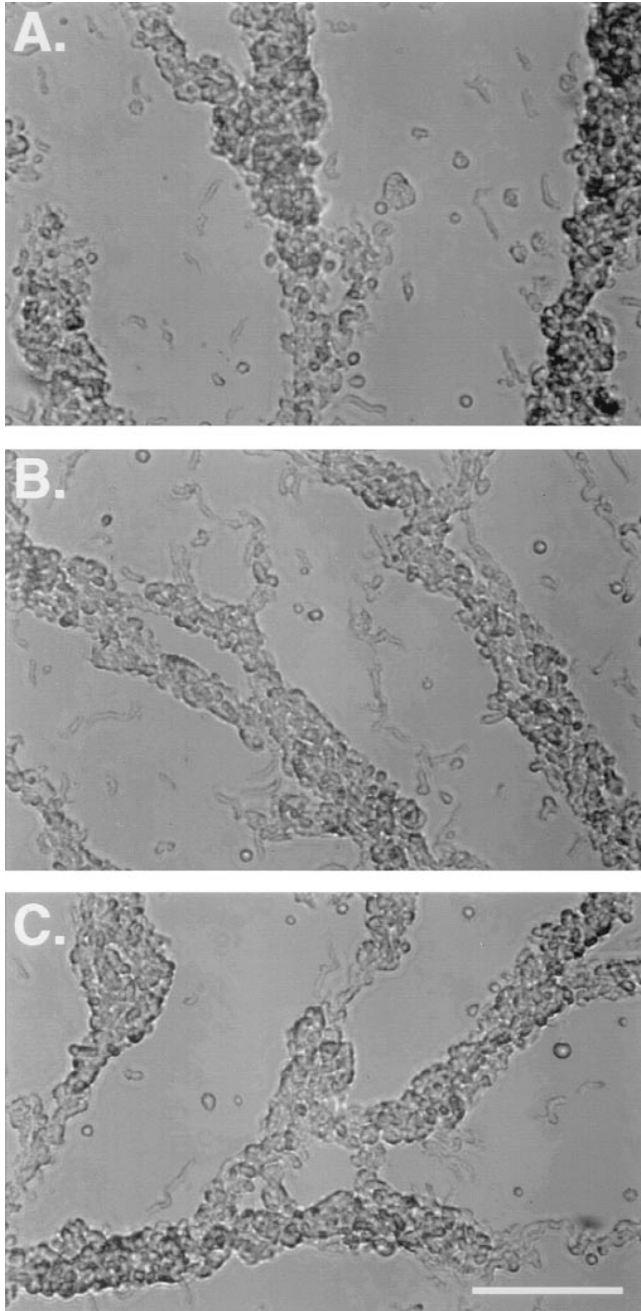


**Figure 4.** The myoB/SH3<sup>-</sup> and S332A-myoB cells undergo normal streaming. The results of a streaming assay on myoB/SH3<sup>-</sup> and S332A-myoB cells. Ax3 cells (A), myoB/SH3<sup>-</sup> cells (B), and S332A-myoB cells (C) photographed at 8 h after starvation. All three cell lines have become elongate and are streaming at this time point. Bar, 100  $\mu$ m.

Random fields of each cell line stained for myoB were chosen to determine the proportion of cells exhibiting the myoB rim staining (Fig. 7, B and C). A total of 100 cells of each strain were randomly chosen, and the number of cells with a full peripheral band of myoB staining was counted. 3% of the Ax3, 80% of the myoB<sup>+</sup>, and 70% of the myoB/SH3<sup>-</sup> cells had a bright peripheral band of myoB staining. Because of the unevenness of the S332A-myoB peripheral stain, we were

unable to accurately assess the number of cells with a true peripheral band of stain.

#### *F-Actin Distribution and Gross Morphology Are Altered in the myoB<sup>+</sup> Cells*

The decreased motility and inability of the myoB<sup>+</sup> cells to become elongate, coupled with the cortical accumulation of myoB, suggested that these mutants were defective in the function of their actin cytoskeleton. The F-actin distribution in the myoB<sup>+</sup>, the myoB/SH3<sup>-</sup>, and the S332A-myoB cells after attachment to a substrate was examined by rhodamine phalloidin staining. Ax3 cells taken from suspension cultures and allowed to attach to coverslips for 10 min begin to spread over the surface and localize F-actin to a thin, peripheral band around the base of the cells (Fig. 8 A, arrow) (Fukui et al., 1991; Peterson and Titus, 1994; Novak et al., 1995). A much broader band of F-actin staining is observed at the base of the myoB<sup>+</sup> cells (Fig. 8 C, arrow). The thick peripheral band of F-actin is observed at every plane of focus throughout the cell (data not shown). The distribution of F-actin at the base of the myoB/SH3<sup>-</sup> and S332A-myoB cells closely resembled that of the Ax3 cells. Both the myoB/SH3<sup>-</sup> cells (Fig. 8 E, arrow) and the S332A-myoB cells (Fig. 8 G) possessed a thin, peripheral band of F-actin at the base of the cells.

Differences in the F-actin distribution were also observed at the apical surfaces of the myoB<sup>+</sup> cells. The Ax3 cells each extend several distinct, circular F-actin filled structures (Fig. 8 B, arrow). These structures correspond to crowns, or amebastomes, and myoB has been previously localized to these protrusions (Novak et al., 1995). Such structures were less frequently observed in the myoB<sup>+</sup> cells. Instead, the apical surface of these cells was devoid of F-actin structures except for small clumps of F-actin and a few short microspikes (Fig. 8, compare D and B). The myoB/SH3<sup>-</sup> cells did not possess the numerous short filopodia observed on myoB<sup>+</sup> cells, but exhibited the normal, crown structures observed in the Ax3 cells (Fig. 8, compare B and F). The S332A-myoB cells also localized apical F-actin in normal structures (Fig. 8 H). Taken together, these results showed that cells overexpressing full-length myoB, but not the mutant forms of myoB, were unable to distribute F-actin properly at the periphery or into apical crown structures during attachment to substrate.

The differences in the myosin I double mutant F-actin patterns were reflected in cell morphologies observed by scanning electron microscopy. As previously observed (Novak et al., 1995), Ax3 cells taken from suspension cultures and allowed to adhere to coverslips for 10–15 min were well spread and polarized, forming plasma membrane extensions at the base of cells (Fig. 9 A, arrows). Each Ax3 cell also had several crownlike structures protruding from their apical surface (Fig. 9 A, arrows), also shown in the rhodamine phalloidin staining (Fig. 8 B). The myoB<sup>+</sup> cells, however, were much rounder and had not yet begun to spread or extend membrane at their base by this time (Fig. 9 B). The crown structures present on the Ax3 cells were rarely observed on the myoB<sup>+</sup> cells (Fig. 9, compare A and B), although a small amount of unorganized ruffling activity was observed (Fig. 9 B). The myoB/

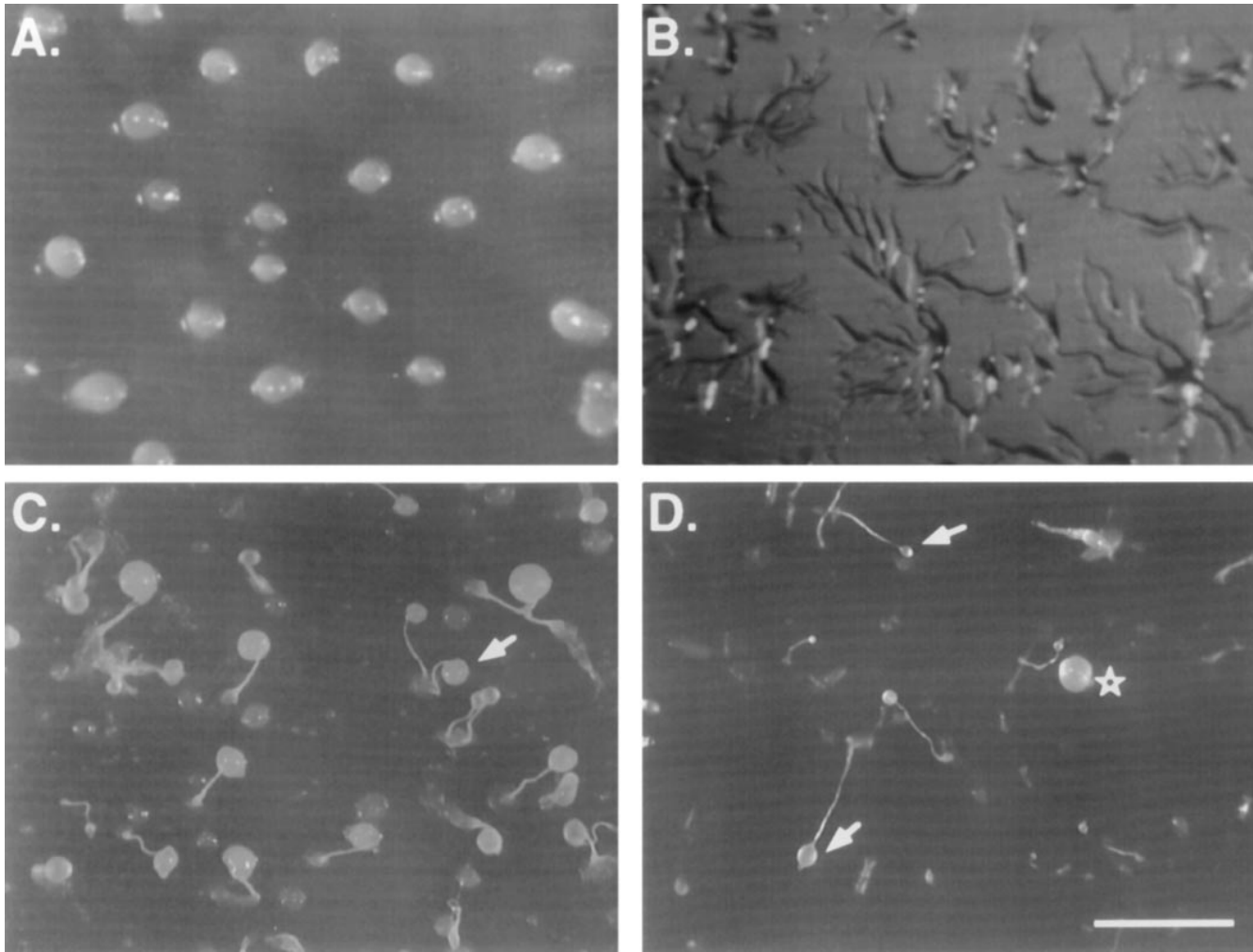


**Figure 5.** The myoB<sup>+</sup> cells undergo abnormal development. The figure shows the development of the myoB<sup>+</sup> cells on nonnutritive agar. The Ax3 (A and C) and myoB<sup>+</sup> cells (B and D) are shown at 12 h (A and B), and 40 h (C and D), after the initiation of starvation. The arrows in C and D point to fruiting bodies. The star in D is placed next to one of the many undeveloped mounds observed for the myoB<sup>+</sup> cells. Bar, 1 mm.

SH3<sup>-</sup> cells and S332A-myoB cells both closely resembled the Ax3 cells. These cells were well extended and polarized, forming normal plasma membrane protrusions and well-organized crown extensions (Fig. 9, C and D, arrows).

#### **The myoB<sup>+</sup> Cells Exhibit Defects in Growth and Pinocytosis**

Another important function of the actin-rich cortex in *Dictyostelium* cells is non-receptor-mediated endocytosis. Cells exhibiting defects in pinocytic activity also have decreased growth rates (Bacon et al., 1994; Novak et al., 1995; Jung et al., 1996). The uptake of FITC-dextran by the suspension-grown myoB<sup>+</sup> cells was analyzed to determine if myoB<sup>+</sup> cells were defective in pinocytosis. Under suspension conditions, control Ax3 cells internalized 0.9  $\mu$ l FITC-dextran/10<sup>6</sup> cells after 60 min (Fig. 10), and an internalization plateau was reached at a final volume of 1.31  $\mu$ l/10<sup>6</sup> cells by 120 min. The myoB<sup>+</sup> cells, however, internalized only 0.3  $\mu$ l FITC-dextran/10<sup>6</sup> cells by 60 min, reaching a plateau at 0.45  $\mu$ l. The suspension-grown myoB/SH3<sup>-</sup>

and S332A-myoB cells did not exhibit any decreased pinocytic activity (Fig. 10). These cells internalized 0.75–0.9  $\mu$ l FITC-dextran/10<sup>6</sup> cells after 60 min (Fig. 10), and plateaued at approximately the same volume as Ax3 cells.

The myoB<sup>+</sup> cells had an increased doubling time when these cells were grown in suspension culture (Table I). The cell number of the Ax3 cells increased every 8 h, saturating at 1  $\times$  10<sup>7</sup> cells/ml, when these cells were grown in suspension. The myoB<sup>+</sup> cell number, however, only doubled once every 20 h in suspension, and growth was saturated at about 5  $\times$  10<sup>6</sup> cells/ml. The myoB/SH3<sup>-</sup> and S332A-myoB cells, in contrast, grew at rates comparable to the parental Ax3 cells (Table I).

#### **Discussion**

The ability to rapidly rearrange the actin network is a prerequisite for cell migration. A key step in translocation is the extension and contraction of pseudopodia. Analysis of *Dictyostelium* mutants overexpressing as little as threefold more of a full-length myosin I (myoB) reveals defects in

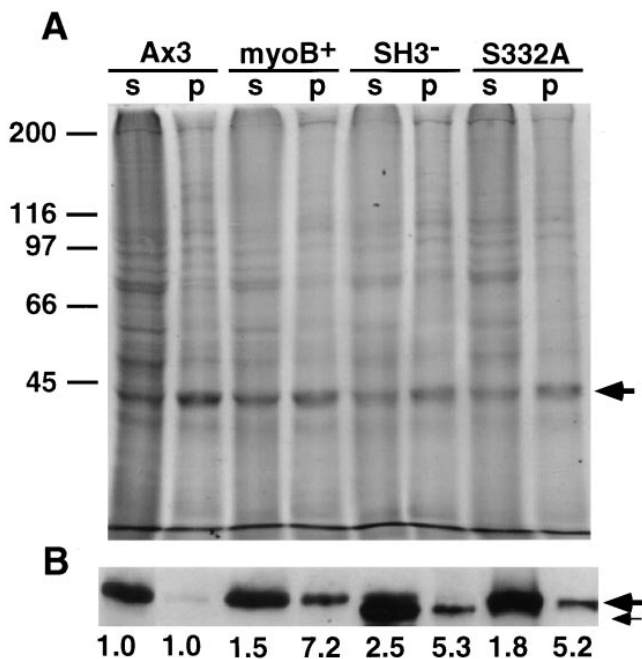


**Figure 6.** An excess of myoB is present in the Triton-insoluble cytoskeletons of myoB<sup>+</sup> cells. Equal numbers of Ax3 myoB<sup>+</sup>, myoB/SH3<sup>-</sup>, and S332A-myoB cells were collected and separated into Triton-soluble fractions (*s*) and Triton-insoluble fractions (*p*). (A) Coomassie blue-stained 12% gel. The arrow indicates the position of the 42-kD F-actin band. The position of the molecular mass standards (kD) are indicated on the left. (B) Western blot of the fractions shown in A. The large arrow indicates the position of the full-length or the overexpressed S332A myoB heavy chain, and the small arrow indicates the position of the truncated myoB/SH3<sup>-</sup> heavy chain. The myoB levels were quantified for each fraction using NIH Image. The value obtained for the myoB band in the Ax3 *s* and *p* lanes were each set to 1.0, and the amount of myoB expressed relative to the wild-type *s* and *p* values is given below each mutant cell fraction in bold.

the formation of plasma membrane extensions and the ability to undergo normal F-actin cytoskeletal rearrangements (Figs. 8 and 9). This disability correlates with a reduced rate of translocation by these cells and impaired development (Figs. 2, 3, and 5). Cells expressing excess amounts of a truncated form of myoB that lacks the SH3 domain or a mutant form of myoB lacking the phosphorylation site do not exhibit the same defects in the actin cortex or cellular behavior as the myoB<sup>+</sup> cells (Figs. 4, 8, and 10), even though the cortical cytoskeletons of all these overexpressing cell lines were found to contain an excess amount of myoB (Fig. 6). The similar localization patterns of overexpressed full-length myoB and mutant forms (Fig. 6) make it unlikely that removal of the SH3 domain or Serine 332 results in improper folding or degradation of the protein. Thus, the disruptive action of the excess myoB in the cell cortex requires that myoB is intact, containing both the SH3 domain at the COOH terminus and the phosphorylation site. These findings are consistent with myosin I playing an important role in actin-based cortical processes required for cell migration that is regulated by intracellular signaling events.

An important question to answer is how a three- to sevenfold excess of a myosin I can have such a significant impact on cortical processes in a *Dictyostelium* cell. The presence of extra full-length myoB in the actin-rich cortex of the cells (Fig. 6) leads to changes in actin staining and in the morphology of the cell (Figs. 8 and 9). There is no apparent overall increase in the amount of actin detected in the Triton-insoluble cytoskeletons (Fig. 6), so it is unlikely that excess actin is being recruited to the cortex. The additional amount of myoB is likely to be excessively cross-linking the cell's cortical F-actin and increasing its binding to the membrane. Recent biochemical studies reveal that myosin I has a small duty cycle or spends most of the time weakly bound to or detached from the actin filament (Ostap and Pollard, 1996). For myosin Is to regulate formation of actin-filled membrane projections, they probably need to be clustered at high concentrations in the cortex. This could be accomplished during myosin I cross-linking of actin filaments and also through localization of myosin I to the plasma membrane. Studies of *Acanthamoeba* myosin I suggest that such conditions exist in vivo (see Discussion in Ostap and Pollard, 1996). The ability of *Acanthamoeba* myosin I to superprecipitate F-actin in vitro demonstrates the ability of myosin Is to perform contractile functions (Fujisaki et al., 1985). Therefore, it is possible that the increased concentration of myoB throughout the cortex of the myoB<sup>+</sup> cells, instead of just at specific regions, would cause these cells to tightly cross-link F-actin all around the periphery. This tightly cross-linked cortex renders the myoB<sup>+</sup> cells unable to extend large, actin-rich projections. The lack of F-actin extensions would then cause the cell's F-actin to become compressed into the thick band observed around the border of the myoB<sup>+</sup> cells (Fig. 8).

The dependence of the overexpression phenotype on the presence of both the myoB SH3 domain and the phosphorylation site suggests that signaling events are required to activate myoB and result in increased tension. The interaction of signaling molecules with the cytoskeleton has been shown to be mediated through many SH3-containing proteins. For example, a protein that binds to the Abl SH3 domain, 3BP-1, is similar to a region of GAP- $\rho$  (Ciccetti et al., 1992). The Rho and Rac GTP-binding proteins have been implicated in regulation of membrane ruffling and assembly of the cytoskeleton (Ridley et al., 1992). A protein that binds to the SH3 domain of ameboid myosin I, Acan 125, has been identified, but its role is unknown (Xu et al., 1995). While the myosin I SH3 domain is not required for the localization of myoB (Figs. 6 and 7), it could be required to link myoB to another protein necessary for its activation.

A serine/threonine kinase would also be a good candidate for an myoB SH3-binding protein. Myosin I heavy chain kinases (MIHCK) have been shown to be active and present at regions of the cell where myosin Is function (Kulesza-Lipka et al., 1991). Although a *Dictyostelium* myoB kinase has not yet been identified, an MIHCK from *Dictyostelium* has been purified and shown to phosphorylate and activate the Mg<sup>2+</sup> ATPase activity of *Dictyostelium* myoD (Lee and Côté, 1995). Cloning and sequencing of this kinase, as well as a MIHCK from *Acanthamoeba*, revealed that they are both members of the protein kinase family that includes the *Saccharomyces cerevisiae* Ste20p and the mammalian p21-activated kinase

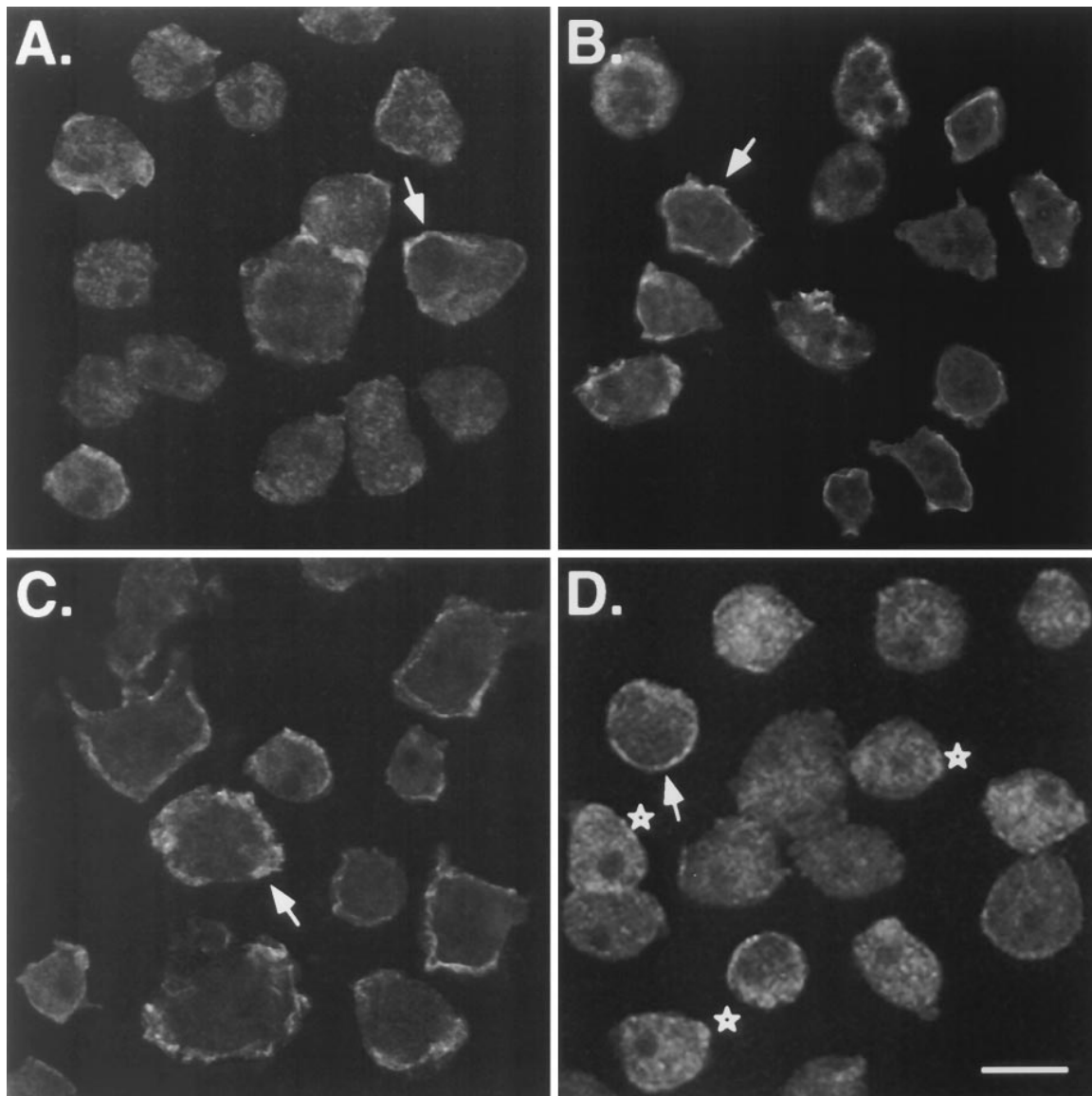


**Figure 7.** An excess of myoB is localized to the periphery of the myoB<sup>+</sup> and myoB/SH3<sup>-</sup> cells. The localization of myoB in the Ax3 (A), myoB<sup>+</sup> (B), myoB/SH3<sup>-</sup> (C), and S332A-myoB (D) cells taken from suspension culture and allowed to adhere to a coverslip for 15 min is shown. Confocal images are shown, obtained near the base of cells. The arrow in A shows an Ax3 cell with myoB localized to one side of the cell. The arrows in B, C, and D point to overexpressing cells that exhibit a peripheral band of myoB around the whole cell. The stars in D point to cells with myoB localized to peripheral regions. Bar, 10  $\mu$ m.

(Brzeska et al., 1996; Lee et al., 1996). Additionally, the *Dictyostelium* MIHCK contains multiple proline-rich sequences potentially able to bind SH3 domains and was shown to contain binding sites for the small G-proteins Cdc42 and Rac 1. Cdc42 and Rac were shown to bind the *Dictyostelium* MIHCK and stimulate its activity (Lee et al., 1996), making MIHCK a potential direct link between Cdc42 signaling pathways and myosin I-mediated cell motility events. The in vivo requirement we have shown for the myoB phosphorylation site and SH3 domain suggest that myoB activity may be regulated via a similar pathway.

An alternate explanation for the myoB overexpression phenotype is that the excess amount of the myoB SH3 domain itself at the cortex interrupts a non-myosin I-related signaling pathway by binding and keeping other SH3-

interacting proteins from their proper targets, thereby disrupting normal cortical rearrangements. This is unlikely as the presence of excess cortical S332A-myoB, which contains the full SH3 domain, does not result in any phenotypic abnormalities. Also, binding of SH3 domains to their targets appears to be a highly specific event. Analysis of phage-displayed peptide libraries has shown that different SH3 domains prefer peptide ligands with specific sequence characteristics and that SH3 domains can discern subtle differences in the primary structure of potential ligands (Rickles et al., 1995; Sparks et al., 1996). Therefore, binding of myoB to its target through the SH3 domain is likely to be a specific interaction, and the overexpression phenotype is not due to an inappropriate stimulation of unrelated SH3 signaling pathways.

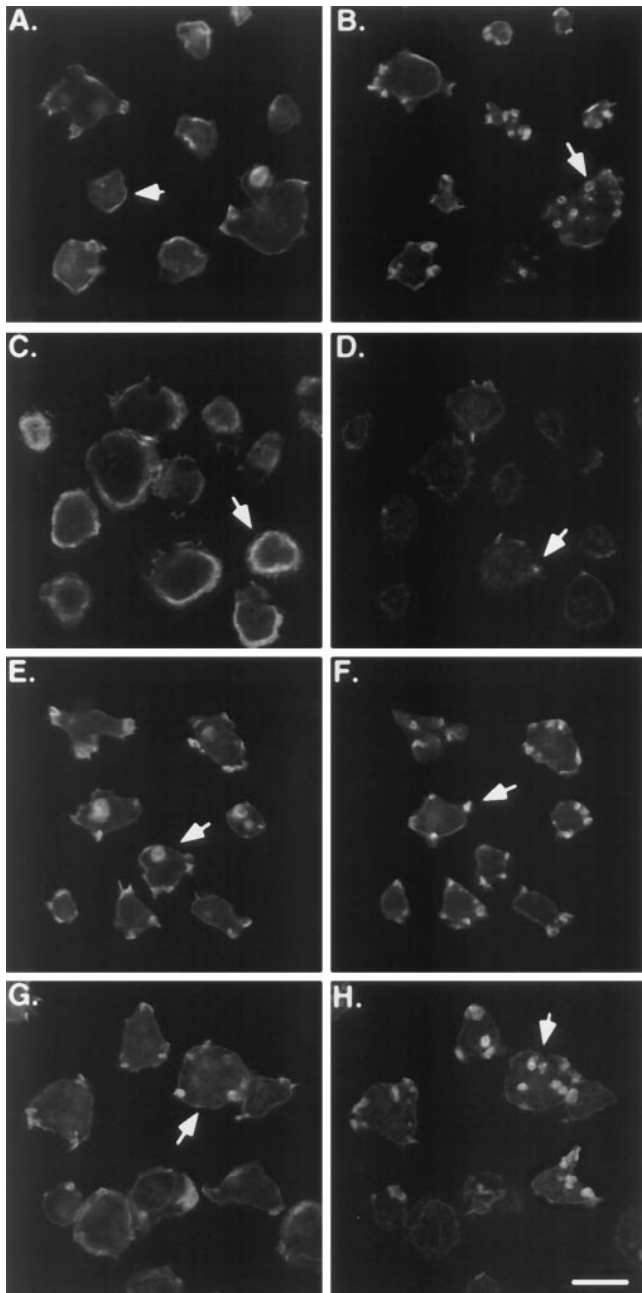


**Figure 8.** The *myoB*<sup>+</sup> cells undergo abnormal F-actin cytoskeletal rearrangements. Shown are confocal images of rhodamine-phalloidin stained cells that have been allowed to attach to a substrate for 10 min. Images of the bottom (A, C, E, and G) and top (B, D, F, and H) of the cells are presented. The pattern of F-actin distribution in the Ax3 (A and B), *myoB*<sup>+</sup> (C and D), *myoB*/*SH3*<sup>-</sup> (E and F), and S332A-*myoB* (G and H) strains are shown. Examples of the peripheral band staining at the base of the cells (A, C, E, and G) and apical crowns (B, F, and H), or small apical clumps of F-actin (D) are indicated with arrows. Bar, 10  $\mu$ m.

The full-length and the unphosphorylated forms of *myoB* are both recruited to the cell periphery, as determined by analysis of S332A-*myoB* Triton-insoluble cytoskeletons (Fig. 6). However, the S332A-*myoB* was observed to be unevenly distributed around the periphery during immunofluorescence (Fig. 7). In *Acanthamoeba*,

total myosin IB was shown to be evenly distributed at the plasma membrane, while phosphomyosin IB was concentrated in specific regions, which corresponded to regions of pinocytosis, phagocytosis, and pseudopodial extension (Baines et al., 1995). One explanation for the incomplete *myoB* staining at the periphery of the S332A-*myoB* cells could be that in *Dictyostelium* phosphorylated and unphosphorylated forms of myosin Is are also differentially distributed around the plasma membrane.

The phenotypic defects observed in the *myoB*<sup>+</sup> cells are distinct from those exhibited by *Dictyostelium* myosin I single and double null mutants. The *myoA*<sup>-</sup> and *myoB*<sup>-</sup> mutants extend an excess of lateral pseudopodia and move with a 50% reduced instantaneous velocity (Wessels et al., 1991, 1996; Titus et al., 1993). Double mutants move with a speed close to that of the single mutants (Novak et al., 1995; Jung et al., 1996) and they extend an excess number of crownlike structures on their ventral surface (Novak et al., 1995). The *myoB*<sup>+</sup> cells appear to be incapable of extending normal actin-rich processes, such as crowns and broad lamellae (Figs. 7 and 8), and they have a more significant decrease in the speed of translocation (Table I) than the myosin I deletion mutants. The developmental defects observed in the *myoB*<sup>+</sup> cells are also more severe than those observed in the myosin I deletion mutants. The *myoB*<sup>+</sup> cells require longer to complete development, and a high proportion of the population is not included in formation of a fruiting body (Fig. 4), while the myosin I deletion mutants develop fruiting bodies that are smaller and less numerous (Jung and Hammer, 1990; Titus et al., 1993; Novak et al., 1995). The one aspect of behavior that is common to the myosin I double mutants and the *myoB*<sup>+</sup> cells is a decreased rate of pinocytosis and slower growth rate (Table I) (Novak et al., 1995; Jung et al., 1996). Phenotypes similar to *myoB* overexpression in *Dictyostelium* have not been observed in mammalian cells where either full-length or truncated brush border myosin I, or the rat *myr1* or *myr2* myosin I tail domains were overexpressed (Ruppert et al., 1995; Durrbach et al., 1996).

The analysis of the myosin I single and double mutant phenotypes led us to propose that these motors, anchored in the plasma membrane of projections or in the underlying cortex, play an important role in retracting actin-rich membrane projections and also provide a contractile force at the membrane-cortex boundary that could inhibit extension of processes. The phenotype of the *myoB*<sup>+</sup> cells is consistent with this model; these cells appear to be overly retracting extensions and tightly restraining the cell cortex. The *myoB*<sup>+</sup> cells do not form large plasma membrane extensions during attachment or become as elongate as Ax3 cells during streaming (Figs. 3 and 8). The only protrusions observed on the *myoB*<sup>+</sup> cells were small filopodia. These may be formed at areas of the actin meshwork that are momentarily relaxed enough to allow the barbed end of actin filaments to push the membrane outward. However, because the F-actin is probably quickly retracted by the excess *myoB* at the point of extension, small protrusions do not have enough time to stabilize into structures such as crowns or pseudopods.

Alterations in the expression levels of other actin-binding proteins also lead to defects in the actin arrangement and cell motility. *Dictyostelium* cells under- or overexpres-

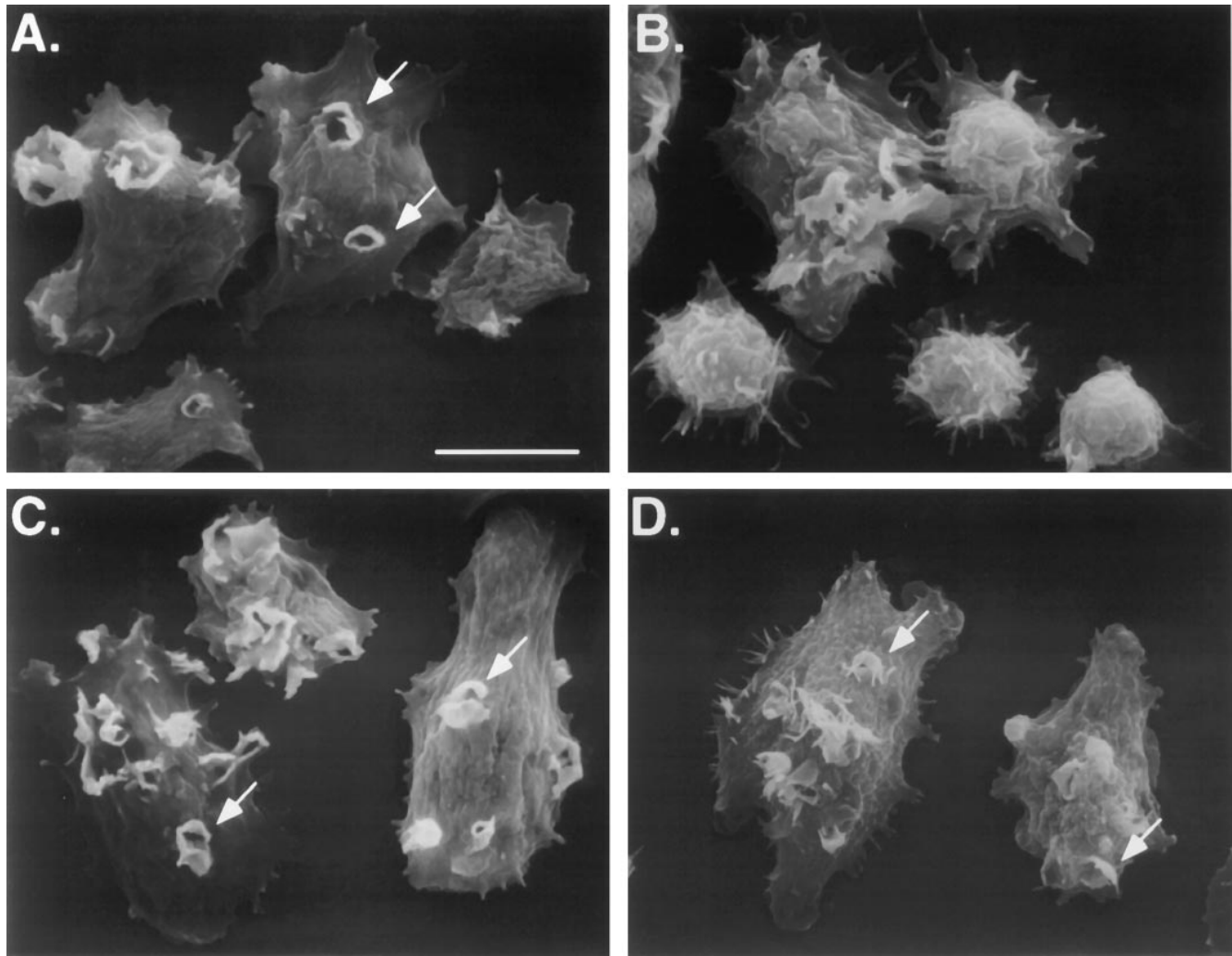


**Figure 9.** The myoB<sup>+</sup> cells exhibit an altered external morphology. Scanning electron micrographs of Ax3 (A), myoB<sup>+</sup> (B), myoB/SH3<sup>-</sup> (C), and S332A-myoB (D) strains grown in suspension culture and allowed to attach to coverslips are presented. Arrows indicate crowns in A, C, and D. Bar, 10  $\mu$ m.

sing capping protein, a protein that caps the barbed ends of actin filaments (Hug et al., 1995), showed differences in actin filament spacing and the number of surface projections. As a result, capping protein underexpressers moved more slowly, while overexpressers increased their velocity (Hug et al., 1995). Overexpression of the actin-modulating protein cofilin in *Dictyostelium* resulted in cells with an increased amount of F-actin, an increased number of actin bundles, and enhanced cell movement (Aizawa et al., 1996). In CV1 cells, overexpression of as little as a 1.4-fold excess of CapG, an actin filament end capping protein, resulted in extensive actin depolymerization at the cell center, increased rates of chemotaxis and cell migration, and formation of more circular dorsal membrane ruffles (Sun et al., 1995). Taken together, these studies revealed that slight changes in the amount of actin-binding proteins present in the cell can affect the entire organizational state of the actin network, and ultimately, the cell's ability to translocate.

The *in vivo* requirement for the SH3 domain in myoB activation supports the hypothesis that myosin Is serve as cytoskeletal effectors linked to signaling molecules. Fur-

ther research into the factors that interact with the myosin I SH3 domain (Xu et al., 1995) as well as other conserved regions of myosin Is will help us understand how these motors are effectively localized and activated. Studies into the function and regulatory mechanisms of myoB have provided further evidence for the importance of myosin Is in controlling reorganization of the F-actin cytoskeleton. Many studies have shown that cells unable to form a cytoskeletal network containing the proper number, distribution and tension of actin filaments cannot extend the correct number or size of membrane processes or undergo normal actin-based cell movements (Cox et al., 1995; Aizawa et al., 1996; Faix et al., 1996). Cytoskeletal proteins such as myosin Is and other actin-binding proteins are likely to work as a tightly regulated team to control the location and timing of cellular projections required for basic cell functions such as endocytosis and locomotion. The amount and distribution of these proteins at the cortex are likely to change in response to different cellular stimuli, such as attachment of bacteria, loss of nutrients, or recognition of a chemotactic signal.

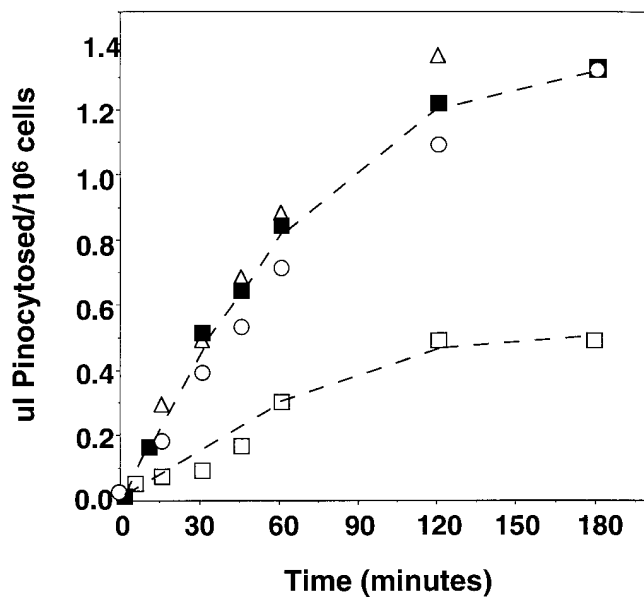


**Figure 10.** The myoB<sup>+</sup> cells are defective in fluid-phase pinocytosis. The uptake of FITC-dextran uptake ( $\mu\text{l}$  pinocytosed/ $10^6$  cells) was measured during the course of 3 h for Ax3 (closed box), myoB/SH3<sup>-</sup> (open triangle), S332A-myoB (open circle) and myoB<sup>+</sup> (open box) cells while in suspension.

Thanks to Dr. Dan Kiehart for many helpful discussions and for critically reading the manuscript. We would like to thank Jon Robertson of the DCMB Group DNA Synthesis Facility for the speedy production of oligos, Dr. Bruce Patterson (University of Arizona, Tucson, AZ) for providing the pBIG, pLittle, and pSmall vectors, and Dr. Angelika Noegel (Max Planck Institute für Biochemie, Martinsried, Germany) for the plasmid pDRH. We would also like to thank Dr. Mike Sheetz for his continuing support and encouragement.

The initial portions of this work were supported by grants from the American Cancer Society (CB-90A and JFRA no. 378), and subsequently by the March of Dimes (no. 1-FY95-0754) and the National Science Foundation (MCB-9507376). M.A. Titus is a member of the Duke Comprehensive Cancer Center.

Received for publication 14 May 1996 and in revised form 1 December 1996.

**Table I. *Dictyostelium myoB* Mutant Phenotypes**

Cell line	Suspension doubling	Streaming time	Instantaneous velocity (percent wild-type) <sup>  </sup>
	<i>h</i>	<i>h</i>	
Ax3*§§	9	8	100
myoB <sup>-</sup> *‡	10.5	10	50
myoA/B <sup>-</sup> §	22	10	58
myoB/C <sup>-</sup> §	24	10	59
myoB <sup>+</sup>	20	14	38
myoB/SH3 <sup>-</sup>	9	8	ND
S332A-myoB	9	8	ND

The data shown are compiled from this paper, Jung & Hammer, 1990 (\*), Wessels et al., 1991 (†), and Novak et al., 1995 (§).

<sup>||</sup>Note that the myoB<sup>+</sup> velocity was obtained from cells at the ripple stage during the streaming assay where the value obtained for the wild-type Ax3 cells was  $17.43 \pm 5.86 \mu\text{m}/\text{min}$ . All other velocities were measured from cells collected at the ripple stage of development on black pads (Wessels et al., 1991) and compared to the velocity of Ax3 cells ( $10.4 \pm 3.1 \mu\text{m}/\text{min}$ ) prepared in the same manner.

## References

- Aizawa, H., K. Sutoh, and I. Yahara. 1996. Overexpression of cofilin stimulates bundling of actin filaments, membrane ruffling, and cell movement in *Dictyostelium*. *J. Cell Biol.* 132:335–344.
- Bacon, R.A., C.J. Cohen, D.A. Lewin, and I. Mellman. 1994. *Dictyostelium discoideum* mutants with temperature-sensitive defects in endocytosis. *J. Cell Biol.* 127:387–399.
- Baines, I.C., H. Brzeska, and E.D. Korn. 1992. Differential localization of *Acanthamoeba* myosin I isoforms. *J. Cell Biol.* 119:1193–1203.
- Baines, I.C., A. Corigliano-Murphy, and E.D. Korn. 1995. Quantification and localization of phosphorylated myosin I isoforms in *Acanthamoeba castellanii*. *J. Cell Biol.* 130:591–603.
- Brzeska, H., and E.D. Korn. 1996. Regulation of class I and class II myosins by heavy chain phosphorylation. *J. Biol. Chem.* 271:16983–16986.
- Brzeska, H., J. Szczepanowska, J. Hoey, and E.D. Korn. 1996. The catalytic domain of *Acanthamoeba* myosin I heavy chain kinase. II. Expression of active catalytic domain and sequence homology to p21-activated kinase (PAK). *J. Biol. Chem.* 271:27056–27062.
- Ciccetti, P., B.J. Mayer, G. Thiel, and D. Baltimore. 1992. Identification of a protein that binds to the SH3 region of Abl and is similar to Bcr and GAP-rho. *Science (Wash. DC)*. 257:803–806.
- Cohen, S.M., D. Knecht, H.F. Lodish, and W.F. Loomis. 1986. DNA sequences required for expression of a *Dictyostelium* actin gene. *EMBO (Eur. Mol. Biol. Organ.) J.* 5:3361–3366.
- Condeelis, J. 1993. Understanding the cortex of crawling cells: insight from *Dictyostelium*. *Trends Cell Biol.* 3:371–376.
- Côté, G.P., J.P. Albanesi, T. Ueno, J.A. Hammer III, and E.D. Korn. 1985. Purification from *Dictyostelium discoideum* of a low-molecular weight myosin that resembles myosin I from *Acanthamoeba castellanii*. *J. Biol. Chem.* 260:4543–4546.
- Cox, D.J., A. Ridsdale, J. Condeelis, and J. Hartwig. 1995. Genetic deletion of ABP-120 alters the three-dimensional organization of actin filaments in *Dictyostelium* pseudopods. *J. Cell Biol.* 128:819–835.
- Drubin, D.G., J. Mulholland, Z. Zhu, and D. Botstein. 1990. Homology of a yeast actin binding protein to signal transduction proteins and myosin I. *Nature (Lond.)*. 343:228–290.
- Durrbach, A., K. Collins, P. Matsudaira, D. Louvard, and E. Coudrier. 1996. Brush border myosin I truncated in the motor domain impairs the distribution and the function of endocytic compartments in a hepatoma cell line. *Proc. Natl. Acad. Sci. USA*. 93:7053–7058.
- Echeverri, C.J., B.M. Paschal, K.T. Vaughan, and R.B. Vallee. 1996. Molecular characterization of the 50-kD subunit of dynactin reveals function for the complex in chromosome alignment and spindle organization during mitosis. *J. Cell Biol.* 132:617–633.
- Egelhoff, T.T., S.S. Brown, and J.A. Spudich. 1991. Spatial and temporal control of nonmuscle myosin localization: identification of a domain that is necessary for myosin filament disassembly in vivo. *J. Cell Biol.* 112:677–688.
- Faix, J., G. Gerisch, and A.A. Noegel. 1992. Overexpression of the cSA cell adhesion molecule under its own cAMP-regulated promoter impairs morphogenesis in *Dictyostelium*. *J. Cell Sci.* 102:203–214.
- Faix, J., M. Steinmetz, H. Boves, R.A. Kammerer, U.M. Lottspeich, J. Murphy, A. Stock, U. Aebi, and G. Gerisch. 1996. Cortaxillins, major determinants of cell shape and size, are actin bundling proteins with a parallel coiled-coil tail. *Cell*. 86:631–642.
- Fujisaki, H., J.P. Albanesi, and E.D. Korn. 1985. Experimental evidence for the contractile activities of *Acanthamoeba* myosins-IA and myosin-IB. *J. Biol. Chem.* 260:1183–1189.
- Fukui, Y., T.J. Lynch, H. Brzeska, and E.D. Korn. 1989. Myosin I is located at the leading edge of locomoting *Dictyostelium* amoebae. *Nature (Lond.)*. 341:328–331.
- Fukui, Y., J. Murray, K.S. Riddelle, and D.R. Soll. 1991. Cell behavior and actomyosin organization in *Dictyostelium* during substrate exploration. *Cell Struct. Funct.* 16:289–301.
- Herskowitz, I. 1987. Functional inactivation of genes by dominant negative mutations. *Nature (Lond.)*. 329:219–222.
- Howard, P.K., K.G. Ahern, and R.A. Firtel. 1988. Establishment of a transient expression system for *Dictyostelium discoideum*. *Nucleic Acids Res.* 16:2613–2623.
- Hug, C., P.Y. Jay, I. Reddy, J.G. McNally, P.C. Bridgman, E.L. Elson, and J.A. Cooper. 1995. Capping protein levels influence actin assembly and cell motility in *Dictyostelium*. *Cell*. 81:1–20.
- Jung, G., and J.A. Hammer III. 1990. Generation and characterization of *Dictyostelium* cells deficient in a myosin I heavy chain isoform. *J. Cell Biol.* 110:1955–1964.
- Jung, G., C.L. Saxe III, A.R. Kimmel, and J.A. Hammer III. 1989. *Dictyostelium discoideum* contains a gene encoding a myosin I heavy chain isoform. *Proc. Natl. Acad. Sci. USA*. 86:6186–6190.
- Jung, G., Y. Fukui, B. Martin, and J.A. Hammer III. 1993. Sequence, expression pattern, intracellular localization and targeted disruption of the *Dictyostelium* myosin ID heavy chain isoform. *J. Biol. Chem.* 268:14981–14990.
- Jung, G., X. Wu, and J.A. Hammer III. 1996. *Dictyostelium* mutants lacking multiple classic myosin I isoforms reveal combinations of shared and distinct functions. *J. Cell Biol.* 133:305–323.
- Klein, G., and M. Satre. 1986. Kinetics of fluid-phase pinocytosis in *Dictyoste-*

- lium discoideum* amoebae. *BBRC (Biochem. Biophys. Res. Commun.)* 138: 1146–1152.
- Kulesza-Lipka, D., I.C. Baines, H. Brzeska, and E.D. Korn. 1991. Immunolocalization of myosin I heavy chain kinase in *Acanthamoeba castellanii* and binding of purified kinase to isolated plasma membranes. *J. Cell Biol.* 115: 109–119.
- Kuspa, A., and W.F. Loomis. 1992. Tagging developmental genes in *Dictyostelium* by restriction enzyme-mediated integration of plasmid DNA. *Proc. Natl. Acad. Sci. USA* 89:8803–8807.
- Lee, S., T.T. Egelhoff, A. Mahasneh, and G.P. Côté. 1996. Cloning and characterization of a *Dictyostelium* myosin I heavy chain kinase activated by Cdc42 and Rac. *J. Biol. Chem.* 271:27044–27048.
- Lee, S.F., and G.P. Côté. 1995. Purification and characterization of a *Dictyostelium* protein kinase required for the actin activation of the  $Mg^{2+}$  ATPase activity of *Dictyostelium* myosin ID. *J. Biol. Chem.* 270:11776–11782.
- Leiting, B., and A.A. Noegel. 1991. The *Ble* gene of *Streptoalloteichus hindustanus* as a new selectable marker for *Dictyostelium discoideum* confers resistance to phleomycin. *BBRC (Biochem. Biophys. Res. Commun.)* 180:1403–1407.
- Lowenstein, E.J., R.J. Daly, W. Li, B. Margolis, R. Lammers, A. Ulrich, E.Y. Skolnik, D. Bar-Sagi, and J. Schlessinger. 1992. The SH2 and SH3 domain-containing protein GRB-2 links tyrosine receptor kinases to ras signaling. *Cell* 70:431–442.
- Mayer, B.J., and D. Baltimore. 1993. Signaling through SH2 and SH3 domains. *Trends Cell Biol.* 3:8–13.
- Novak, K.D., M.D. Peterson, M.C. Reedy, and M.A. Titus. 1995. *Dictyostelium* myosin I double mutants exhibit conditional defects in pinocytosis. *J. Cell Biol.* 131:1205–1221.
- Ostap, E.M., and T.D. Pollard. 1996. Biochemical kinetic characterization of the *Acanthamoeba* myosin I ATPase. *J. Cell Biol.* 132:1053–1060.
- Patterson, B., and J.A. Spudich. 1995. A novel positive selection for identifying cold-sensitive myosin II mutants in *Dictyostelium*. *Genetics* 140:505–515.
- Peterson, M.D., and M.A. Titus. 1994. F-actin distribution of *Dictyostelium* myosin I double mutants. *J. Eukaryot. Microbiol.* 41:652–657.
- Peterson, M.D., K.D. Novak, M.C. Reedy, J.I. Ruman, and M.A. Titus. 1995. Molecular genetic analysis of myoC, a *Dictyostelium* myosin I. *J. Cell Sci.* 108:1093–1103.
- Pollard, T.D., S.K. Doberstein, and H.G. Zot. 1991. Myosin I. *Annu. Rev. Physiol.* 53:653–681.
- Rickles, R.J., M.C. Botfield, X. Zhou, P.A. Henry, J.S. Brugge, and M.J. Zoller. 1995. Phage display selection of ligand residues important for Src homology 3 domain binding specificity. *Proc. Natl. Acad. Sci. USA* 92:10909–10913.
- Ridley, A.J., H.F. Paterson, C.L. Johnston, D. Diekmann, and A. Hall. 1992. The small GTP-binding protein *rac* regulates growth factor-induced membrane ruffling. *Cell* 70:401–410.
- Ruppert, C., R. Kroschewski, and M. Bähler. 1993. Identification, characterization and cloning of myr1, a mammalian myosin-I. *J. Cell Biol.* 120:1393–1403.
- Ruppert, C., J. Godel, R.T. Müller, R. Kroschewski, J. Reinhard, and M. Bähler. 1995. Localization of the rat myosin I molecules myr 1 and 2 and in vivo targeting of their tail domains. *J. Cell Sci.* 108:3775–3786.
- Sparks, A.B., J.E. Rider, N.G. Hoffman, D.M. Fowlkes, L.A. Quilliam, and B.K. Kay. 1996. Distinct ligand preferences of Src homology 3 domains from Src, Yes, Cortactin, p53bp2, PLC $\gamma$ , Crk, and Grb2. *Proc. Natl. Acad. Sci. USA* 93:1540–1544.
- Spudich, A. 1987. Isolation of the actin cytoskeleton from ameboid cells of *Dictyostelium*. *Methods. Cell Biol.* 28:209–214.
- Spudich, J.A. 1982. *Dictyostelium discoideum*: methods and perspectives for the study of cell motility. *Methods Cell Biol.* 25:359–364.
- Stossel, T.P. 1989. From signal to pseudopod. *J. Biol. Chem.* 264:18261–18264.
- Sun, H.Q., K. Kwiatkowska, D.C. Wooten, and H.L. Yin. 1995. Effects of CapG overexpression on agonist-induced motility and second messenger generation. *J. Cell Biol.* 129:147–156.
- Swanson, J.A., and C. Watts. 1995. Macropinocytosis. *Trends Cell Biol.* 5:424–427.
- Titus, M.A., H.M. Warrick, and J.A. Spudich. 1989. Multiple actin-based motor genes in *Dictyostelium*. *Cell Regul.* 1:55–63.
- Titus, M.A., D. Wessels, J.A. Spudich, and D. Soll. 1993. The unconventional myosin encoded by the *myoA* gene plays a role in *Dictyostelium* motility. *Mol. Biol. Cell.* 4:233–246.
- Titus, M.A., K.D. Novak, G.P. Hanes, and A.S. Urioste. 1995. Molecular genetic analysis of *myoF*, a new *Dictyostelium* unconventional myosin gene. *Biophys. J.* 68:152s–157s.
- Urrutia, R.A., G. Jung, and J.A. Hammer. 1993. The *Dictyostelium* myosin-IE heavy chain gene encodes a truncated isoform that lacks sequences corresponding to the actin-binding site in the tail. *Biochem. Biophys. Acta.* 1173: 225–229.
- Varnum, B., K.B. Edwards, and D.R. Soll. 1986. The developmental regulation of single-cell motility in *Dictyostelium discoideum*. *Dev. Biol.* 113:218–227.
- Wagner, M.C., B. Barylko, and J.P. Albanesi. 1992. Tissue distribution and subcellular localization of mammalian myosin I. *J. Cell Biol.* 119:163–170.
- Wasenius, V.M., O. Narvanen, V.P. Lehto, and M. Saraste. 1987.  $\alpha$ -Actinin and spectrin have common structural domains. *FEBS Lett.* 221:73–76.
- Wessels, D., J. Murray, G. Jung, J.A. Hammer III, and D.R. Soll. 1991. Myosin IB null mutants of *Dictyostelium* exhibit abnormalities in motility. *Cell Motil. Cytoskel.* 20:301–315.
- Wessels, D., M.A. Titus, and D.R. Soll. 1996. A *Dictyostelium* myosin I plays a crucial role in regulating the frequency of pseudopods formed on the substratum. *Cell Motil. Cytoskel.* 33:64–79.
- Wu, L., J. Franke, R.L. Blanton, G.J. Podgorski, and R.H. Kessin. 1995. The phosphodiesterase secreted by prestalk cells is necessary for *Dictyostelium* morphogenesis. *Dev. Biol.* 167:1–8.
- Xu, P., A.S. Zot, and H.G. Zot. 1995. Identification of Acan125 as a myosin-I binding protein present with myosin-I on cellular organelles of *Acanthamoeba*. *J. Biol. Chem.* 270:25316–25319.